NASA TECHNICAL NOTE

NASA TN D-6537
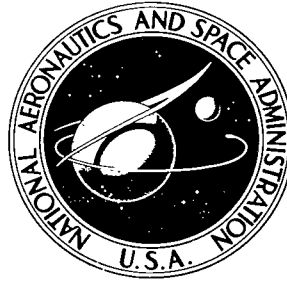
EFFECT OF SEVERAL POROUS CASING TREATMENTS ON STALL LIMIT AND ON OVERALL PERFORMANCE OF AN AXIAL-FLOW COMPRESSOR ROTOR

by Walter M. Osborn, George W. Lewis, Jr., and Laurence J. Heidelberg

Lewis Research Center
Cleveland, Ohio 44135

0133440

1. Report No. NASA TN D-6537	2. Government Accession No.	3. Recipient's Catalog No.
4. Title and Subtitle EFFECT OF SEVERAL POROUS CASING TREATMENTS ON STALL LIMIT AND ON OVERALL PERFORMANCE OF AN AXIAL-FLOW COMPRESSOR ROTOR		5. Report Date November 1971
		6. Performing Organization Code
7. Author(s) Walter M. Osborn, George W. Lewis, Jr., and Laurence J. Heidelberg		8. Performing Organization Report No. E-5973
9. Performing Organization Name and Address Lewis Research Center National Aeronautics and Space Administration Cleveland, Ohio 44135		10. Work Unit No. 720-03
		11. Contract or Grant No.
12. Sponsoring Agency Name and Address National Aeronautics and Space Administration Washington, D.C. 20546		13. Type of Report and Period Covered Technical Note
		14. Sponsoring Agency Code

15. Supplementary Notes

16. Abstract

Several geometrically different porous casings were tested with an axial-flow compressor rotor to determine their effects upon the rotor stall-limit line and overall performance. The tests were conducted using both uniform and nonuniform inlet-flow conditions. The rotor performance with the various casing treatments is compared with that obtained with a solid casing. The ability of the various casing treatments to displace the rotor stall-limit line to lower weight flows was observed. Significant stall-margin increases were obtained with several of the porous casings. Peak efficiencies with two of the porous casings were as high as or slightly higher than that obtained with solid casing.

17. Key Words (Suggested by Author(s)) Compressor casing treatment Stall margin improvement	18. Distribution Statement Unclassified – unlimited

19. Security Classif. (of this report) Unclassified	20. Security Classif. (of this page) Unclassified	21. No. of Pages 47	22. Price* $3.00

CONTENTS

EFFECT OF SEVERAL POROUS CASING TREATMENTS ON STALL LIMIT AND ON OVERALL PERFORMANCE OF AN AXIAL-FLOW COMPRESSOR ROTOR

by Walter M. Osborn, George W. Lewis, Jr., and Laurence J. Heidelberg

Lewis Research Center

SUMMARY

A series of tests were made to evaluate the effect of geometrically different porous casings on the performance of an axial-flow compressor rotor. The tests were conducted using uniform, tip radially distorted, and circumferentially distorted inlet flow conditions. Thirteen porous casings were tested: two perforated casings, three variations of honeycomb, a circumferentially grooved, an axially slotted, two variations of skewed slotted, and four variations of blade angle slotted. The effectiveness of the casing treatments was judged primarily by their ability to maintain or increase the pressure ratio while decreasing the weight flow at the stall-limit point below that obtained for a reference solid casing.

The skewed slotted casing with the slots open to a chamber gave the greatest displacement of the stall-limit line for all speeds tested with both uniform and radially distorted inlet flow. The skewed slotted casing with closed slots also gave a good displacement of the stall-limit line, but the improvement was not as large as it was for the open slots. However, with both skewed slotted configurations the maximum efficiency was significantly lower than that obtained with the solid casing.

Of the four blade angle slotted configurations tested, only the one with closed, shallow, and short slots gave a good displacement of the stall-limit line with uniform inlet flow. This casing and the circumferentially grooved casing gave maximum efficiencies, as high or slightly higher than the reference solid casing, along with a good displacement of the stall-limit line.

The honeycomb casings gave a good displacement of the stall-limit line with efficiencies a little lower than those obtained with the solid casing.

The performance results obtained with the axially slotted casing were inconclusive because of damage to the casing during the tests. However, a good displacement of the stall-limit line is indicated at speeds below 0.9 of design speed.

A small improvement in the location of the stall-limit line was obtained with the perforated casing with large holes but no improvement was obtained with the perforated casing with small holes.

The limited data obtained with circumferentially distorted inlet flow indicated that substantial increases in stall margin might be obtained with casing treatment.

INTRODUCTION

Modern aircraft may be required to operate over a wide range of flight speeds with conditions of varying inlet flow distortions and time-unsteady flow into the engine. Thus, the fan and compressor must be capable of stable operation with these adverse inlet conditions.

In general, improving the flow margin between the fan-compressor operating point and the stall-limit point will also improve the useful operating range of the propulsion system. In the investigation of reference 1, an axial-flow rotor was tested with a porous casing and plenum chamber arrangement ahead of and over the rotor blades. This arrangement was used for external bleed and blow. Increases in flow range and, therefore, stall margin were obtained with both bleeding and blowing. A substantial increase was also noted when no bleeding or blowing was used. In the investigation of reference 2, additional tests without bleeding or blowing were conducted with modifications to the porous casing of reference 1 and various configurations of two more porous casings. Increases in stall margin were obtained in about half of the configurations tested. In both investigations, the stall-margin improvement was greatest when an inlet flow distortion was present. This was attributed to the fact that with distorted flow the blade tip was critical (i.e., rotating stall was first evidenced in the tip region of the rotor). It was felt that the onset of rotating stall was delayed by the porous casing; however, the flow mechanisms associated with the performance improvement were not identifiable.

To further study the effects of casing treatment on rotor performance, an investigation has been made at the NASA Lewis Research Center to evaluate different types of porous casing treatments. Three slotted, several honeycomb, two perforated, and a circumferentially-grooved casing were tested. Based on the results of references 1 and 2, a rotor that was tip critical was selected for testing with these casing treatments. This report presents the overall performance results for uniform inlet-flow conditions for the rotor with a solid casing and with the porous casing treatments. Also presented are the performance results for the rotor with a solid casing and selected porous casing treatments with screen-generated tip radial and circumferential inlet flow distortions.

SYMBOLS

N rotor speed at design condition, rpm

N_D equivalent design speed, $N/\sqrt{\theta}$, 16 000 rpm

W air weight flow, lbm/sec

δ ratio of inlet (plenum) total pressure to NASA standard sea-level pressure of 14. 69 psia

η_{ad} temperature-rise efficiency

θ ratio of inlet (plenum) total temperature to NASA standard sea-level temperature of 518. 7° R

APPARATUS AND PROCEDURE

TEST FACILITY

A schematic diagram of the test facility is shown in figure 1. With the exception of a longer inlet line to accommodate a distortion screen, the facility is the same as that described in reference 3. The drive system consists of a 15 000-horsepower electric motor with a variable-frequency speed control. Motor speed may be controlled from 360 to 3600 rpm. The motor was coupled to a 5. 02 ratio speed-increaser gearbox that drove the test rotor. The working fluid was atmospheric air. The facility was sized for a maximum flow rate of approximately 100 pounds per second. The facility was operated with an exhaust of 26 inches of mercury downstream of the throttle valves. Airflow was controlled by a butterfly valve in the outlet line. A thin-plate orifice, located in the inlet line, was used to determine the airflow. A plenum tank 6 feet in diameter and approximately 12 feet long was located upstream of the test rotor. A bellmouth nozzle was located between the plenum tank and the inlet of the test rotor.

TEST ROTOR

A photograph of the test rotor is shown in figure 2. The rotor had an inlet tip diameter of 19. 77 inches and an outlet tip diameter of 19. 54 inches. The inlet hub-tip radius ratio was 0. 51. The number of blades (47) was selected to provide a solidity of 1. 48 at the rotor tip. The rotor was designed for a tip speed of 1380 feet per second (16 000 rpm). Design weight flow was 65. 3 pounds per second which corresponds to a weight flow per unit annulus area at the rotor leading edge of 41. 2 pounds per second per square foot. The rotor was equipped with blade vibration dampers located at 43 percent of span from the rotor tip. A more detailed description of the test rotor is presented in reference 3.

The test data obtained in reference 3 showed that the rotor was highly loaded in the blade tip region. Therefore, stall might be expected to initiate in the tip regions (tip critical). Thus, this rotor was selected for the casing treatment tests.
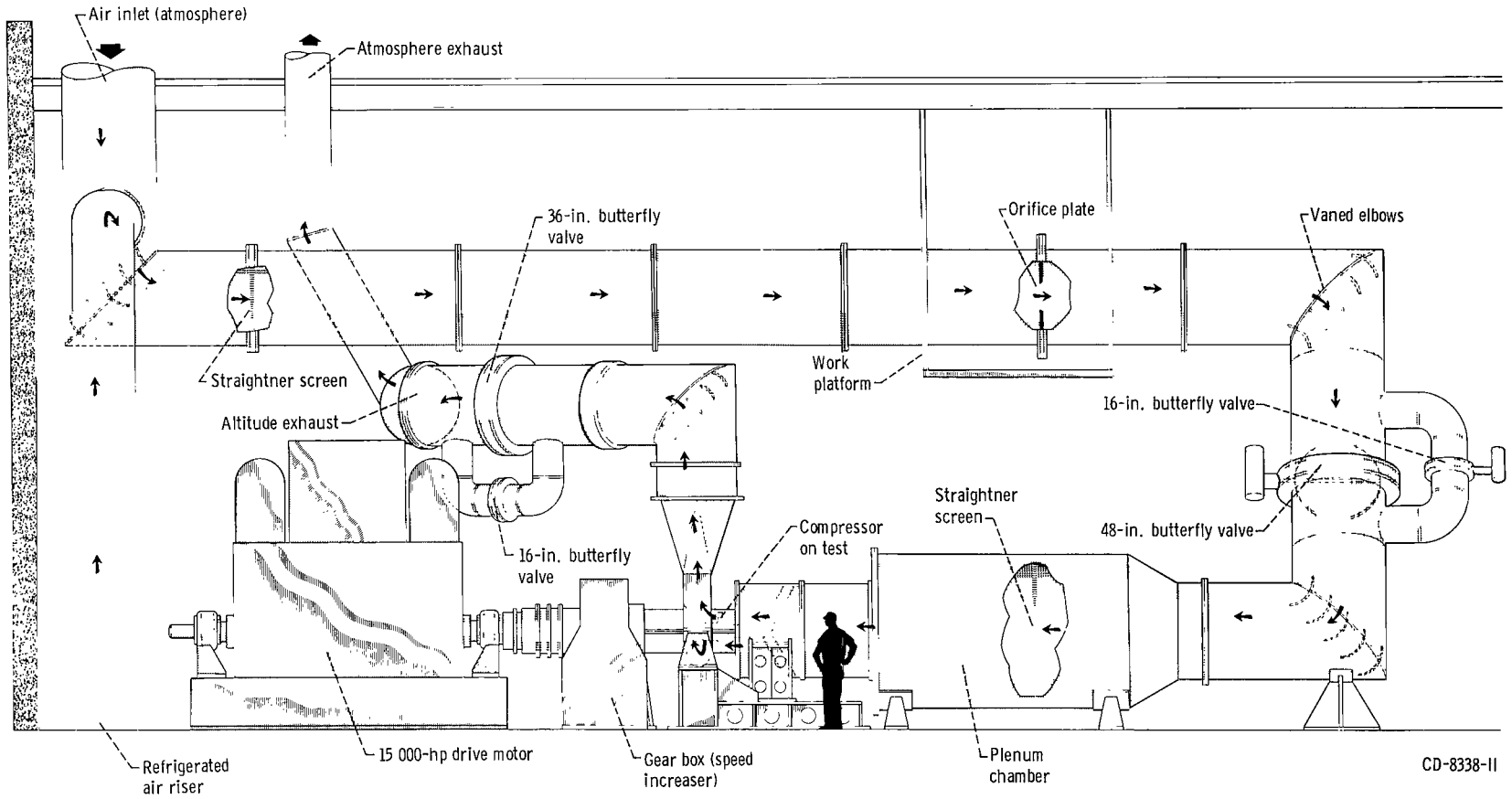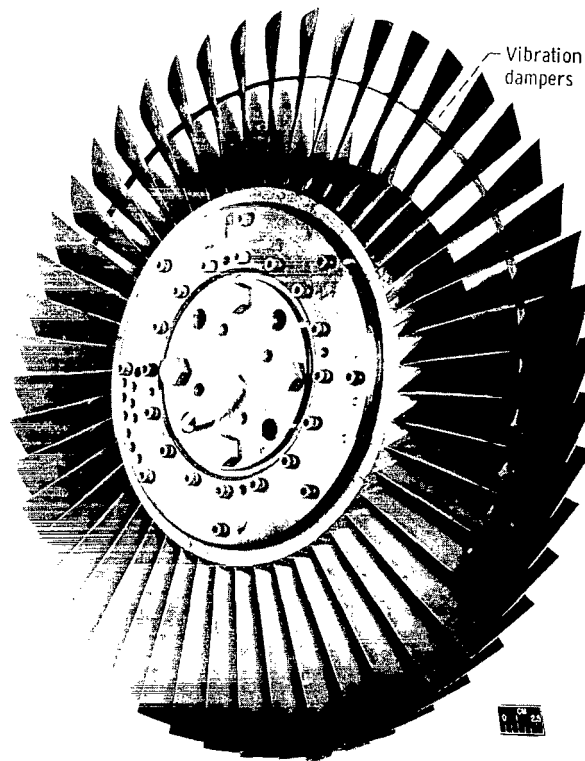
Figure 1. - Compressor test facility.

CD-8338-11

Figure 2. - Test rotor.

C-70-451

CASING TREATMENT CONFIGURATIONS

The following considerations were used in determining the casing treatment designs: (1) porosity or percent open area, (2) acoustical tuning, and (3) recirculation.

The percent open area is the ratio of the total open area to the total treated area over the rotor blade tips. The nominal percent open area chosen was 67 percent, although other values were also used.

Tuning may be associated with the interchange of pressure and flows between the main stream and the porous casing as the outer-wall static pressure is pulsating with respect to time at blade passing frequency. Simple organ pipe theory was used for tuning the passages. A nominal value for tuning was selected to be at a blade passing frequency of $0.9 \ N_D$. Generally, the passage depths were selected for that frequency. The static temperature in the passage was assumed to be equal to the rotor outlet total temperature in order to determine the passage depth. Some of the configurations were tested with both open (to plenum) and closed passages. For the same passage depth, closing the passage lowered the tuning frequency to half the value with open passages.
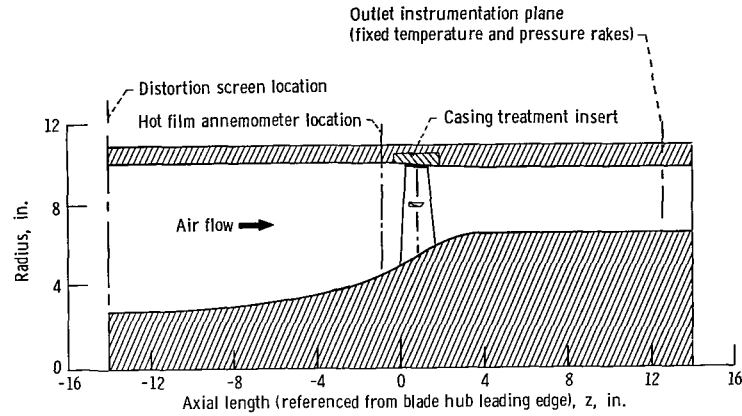
5

Figure 3. - Meridional view of axial-flow rotor showing location of casing treatment insert.

TABLE I. - SUMMARY OF CASING TREATMENTS

Type of insert	Description of casing treatment (in order of discussion)	Nominal open area (percent)	Conditions at back of treatment
Perforated sheet (fig. 4)	(a) 0.0625-in.-diam holes, 0.109 in. between centers	30	Open
	(b) 0.125-in. diam holes, 0.188 in. between centers	40	Open
Honeycomb (fig. 5)	(a) Deep (0.55 in., av)[a], small cell (0.19×0.11 in.)	99	Closed
	(b) Shallow (0.32 in., av)[a], small cell (0.19×0.11 in.)	99	Closed[b]
	(c) Deep (0.55 in., av)[a], large cell (0.33×0.20 in.)	99	Closed
Circumferentially grooved (fig. 6)	Seven grooves, 0.125 in. wide by 0.375 in. deep, 0.062 in. land width	67	Closed
Axially slotted (fig. 7)	576 slots, 0.070 in. wide by 0.64 in. deep (av)[a], 0.035 in. land width	67	Open[b]
Skewed slotted (fig. 8)	(a) 288 slots at 60° angle to radial plane, 0.070 in. wide by 0.64 in. deep (av)[a], 0.035 in. land width	67	Open[b]
	(b) Same as (a) except for conditions at back of slot	67	Closed
Blade angle slotted (fig. 9)	(a) 310 slots alined with average blade setting angle at blade tip; 0.070 in. wide by 0.64 in. (av)[a] deep, 0.035 in. land width; long slots (1.25 in. axial length) extend beyond blade tip inlet and outlet (see fig. 9(a))	67	Open[b]
	(a) Same except for conditions at back of slot	67	Closed
	(b) Same as (a) except for shallow slot depth of 0.32 in. (av)[a] and conditions at back of slot (fig. 9(b))	67	Closed[b]
	(c) Same as (b) except slots were short (0.63 in. axially) (see fig. 9(c))	67	Closed[b]

[a]Depth at center (axially) of insert.
[b]Tuned to approximately 90 percent of blade passing frequency.

Recirculation was considered in two respects: (1) circumferential recirculation between the slot passages and (2) axial recirculation within the individual slots from the downstream high-pressure region to the inlet region. In some of the treatments, a rubber seal was used at the slot outlet to close the slot and eliminate slot to slot recirculation.

The casing treatment configurations were fabricated as inserts to fit in a casing groove over the rotor tip as shown in figure 3. There is a 4° taper on the inner diameter of the insert. The static clearance between the rotor tip and the insert was nominally 0.020 inch.
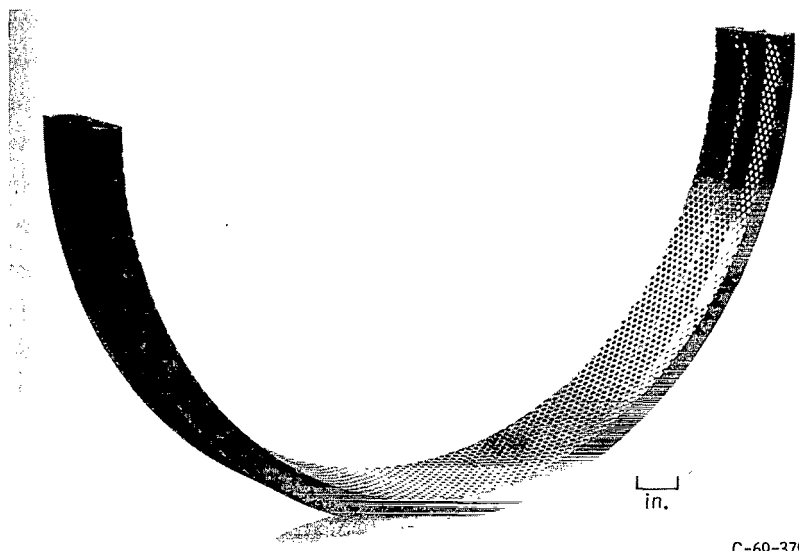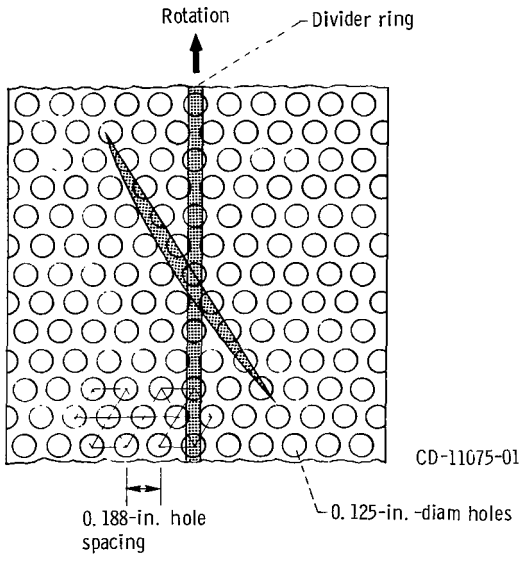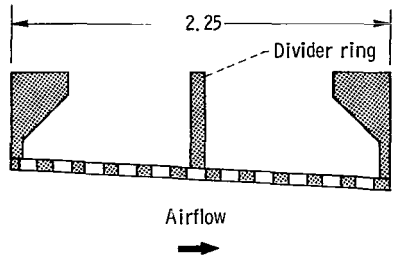
The casing treatments are described in the following sections and a summary is presented in table I.

Perforated Casings

Two different perforated casings were fabricated. One had 0.0625-inch-diameter holes, which accounted for approximately 30 percent of the surface area. The other had 0.125-inch-diameter holes with approximately 40 percent open area (fig. 4). The holes extended the full axial length of the insert and, thus, there was some open area both upstream and downstream of the rotor blades. A plenum existed behind the holes, and a divider ring was located at midspan to limit the recirculation of air from back to front.

Honeycomb Casings

Three honeycomb casing inserts were fabricated. These inserts used two different sizes of cells. The small honeycomb had 0.19- by 0.11-inch cells, and the large honeycomb 0.33- by 0.20-inch cells. A sketch and a photograph of the large cell honeycomb casing insert are shown in figure 5. The small cell honeycomb was tested with two radial depths (table I); only the deep large-cell honeycomb was tested. The shallow small-cell honeycomb was selected for acoustical tuning of the cell to blade passing frequency at $0.9\ N_D$. The aluminum honeycomb was bonded to a steel support ring. Thus, the honeycomb cells were closed, and cell to cell recirculation of the air was minimized. The honeycomb extended the full axial length of the insert with honeycomb cells located upstream of, over, and downstream of the rotor blades (fig. 5).

2.25

Divider ring

Airflow

Rotation — Divider ring

CD-11075-01

0.188-in. hole spacing

0.125-in.-diam holes

C-69-3797

in.

Figure 4. - Perforated casing insert with 0.125-inch-diameter holes. Hole spacing for perforated casing with 0.0625-inch-diameter holes = 0.109 inch.
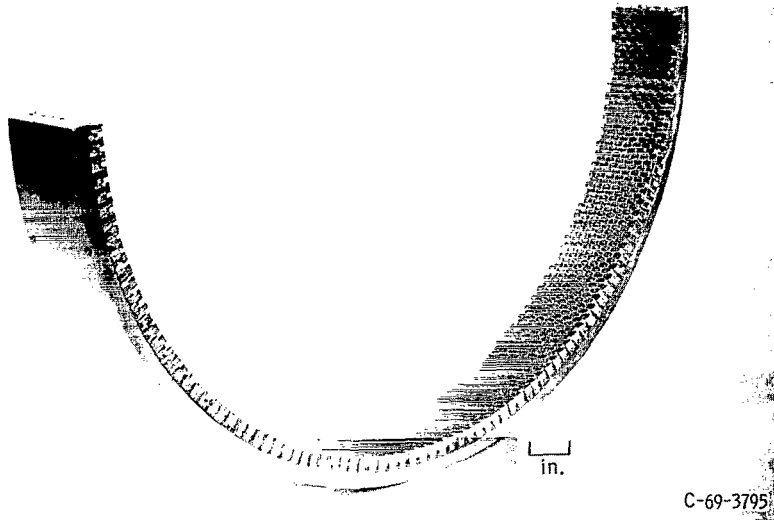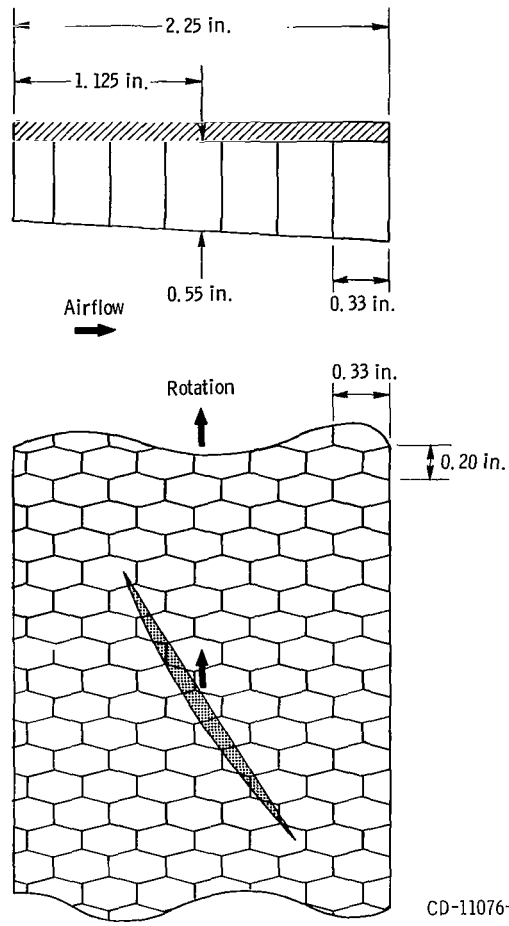
2.25 in.

1.125 in.

0.55 in.

0.33 in.

Airflow

Rotation

0.33 in.

0.20 in.

CD-11076-01

C-69-3795

Figure 5. - Honeycomb casing insert with large cells.

9

Circumferentially Grooved Casing

A sketch and a photograph of the circumferentially grooved casing insert is shown in figure 6. There are seven grooves (each 0.375 in. deep). The first and seventh grooves extend beyond the blade leading edge and blade trailing edge, respectively (fig. 6). The groove (open) area is about two-thirds of the total area as the groove width is twice the land width. The circumferentially grooved casing should eliminate axial recirculation but circumferential recirculation from blade to blade along the grooves is possible.
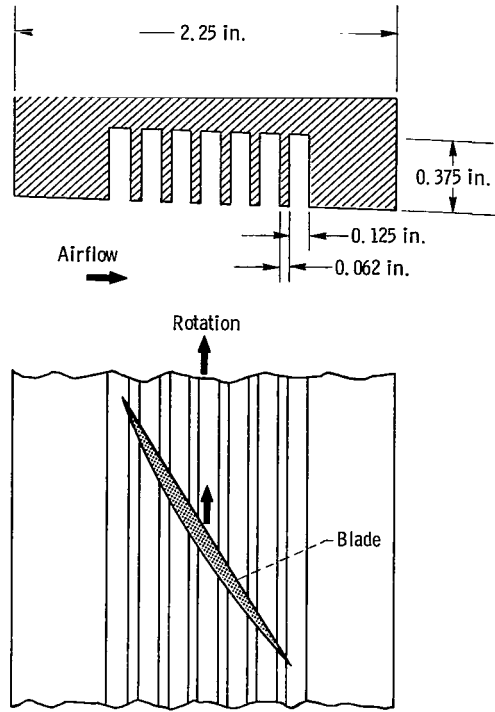
Axially Slotted Casing

Figure 7 shows a sketch and a photograph of the axially slotted casing. The 576 slots are alined in the axial and radial planes with the slot width twice the land width. Thus, the open area is approximately two-thirds of the total area. The slots extend beyond the leading and trailing edges of the rotor blades. The slot depth (average, 0.64 in.) tuned the passage to blade passing frequency at 0.9 N_D. The slot was open to a small plenum (0.030 in. deep).

Skewed Slotted Casing

A sketch and photograph of the skewed slotted casing are shown in figure 8. The slots are alined with the axial plane but are skewed at a 60° angle to the radial plane. The slight angle of the slots to the axial plane shown in figure 8 results from the changing radius of the inner diameter of the insert (fig. 3). There are 288 slots with the slot width twice the land width. Thus, the open area is approximately two-thirds of the total area. The slots extend beyond the leading and trailing edges of the rotor blades. With a slot depth of 0.64 inch and a plenum behind the slots, this configuration is tuned to the blade passing frequency at 0.9 N_D. Although the skewed slot depth is the same as the axial slot depth, a larger plenum (0.30 in. deep) is obtained for the skewed insert than for the axial insert because of the skew angle. This configuration was also tested with the slots closed (rubber seal at slot outlet), which lowers the tuning frequency by one-half.

Blade Angle Slotted Casing

The blade angle slotted casing was tested in four configurations. Only one insert was fabricated, but three modifications were made to the insert. Sketches of the four config-

2.25 in.

0.375 in.

0.125 in.

0.062 in.

Airflow

Rotation

Blade

CD-11077-01

in.
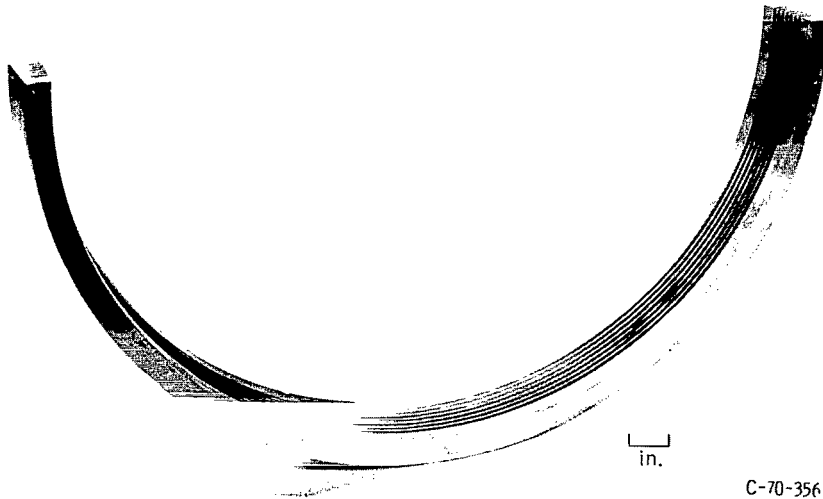
C-70-356

Figure 6. – Circumferentially grooved casing insert.

11

2.25 in.

0.030 in.

0.64 in.

Airflow

1.25 in.

Rotation

0.035 in.

0.070 in.
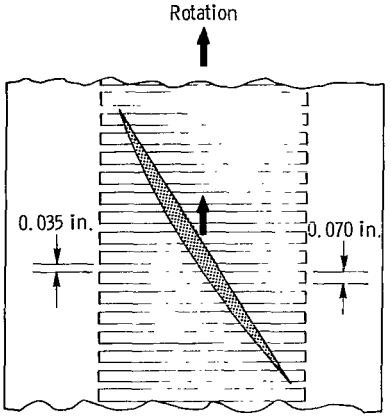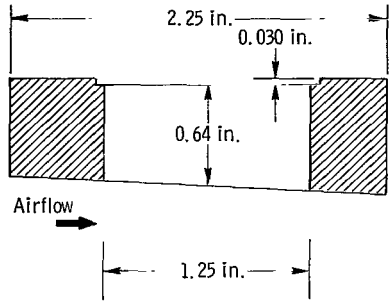
CD-11078-01
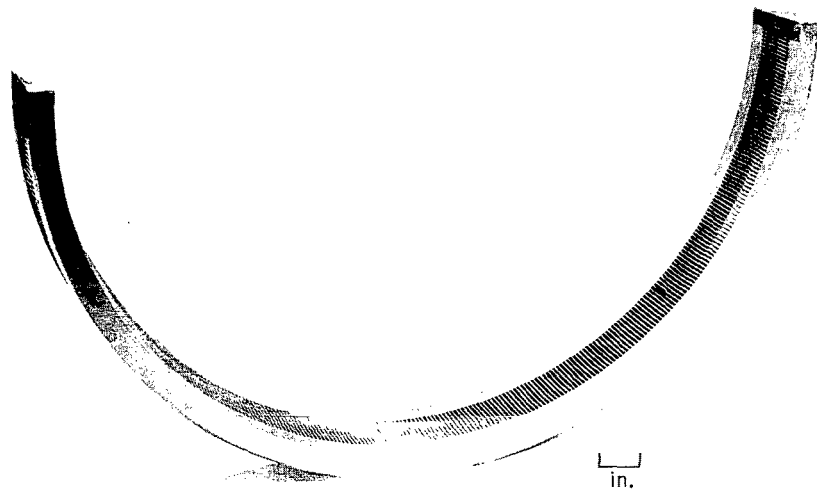
C-70-357

Figure 7. – Axially slotted casing insert.

2.25 in.

Backing plate

Rubber seal

1.25 in.

Airflow

Rotation

0.640 in.

0.070 in.

0.035 in.

60°

Rotation

CD-11079-01

in.
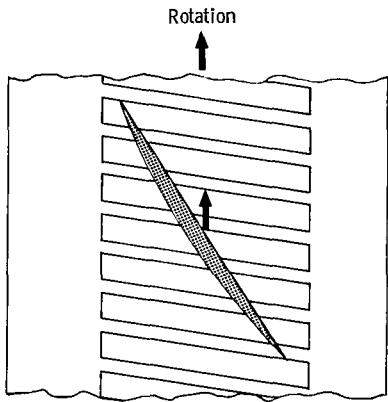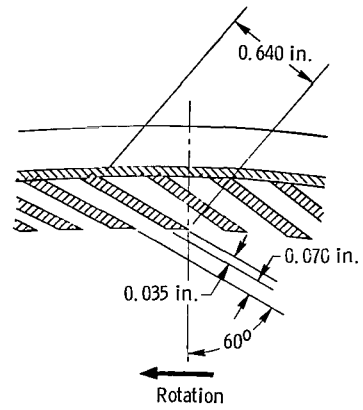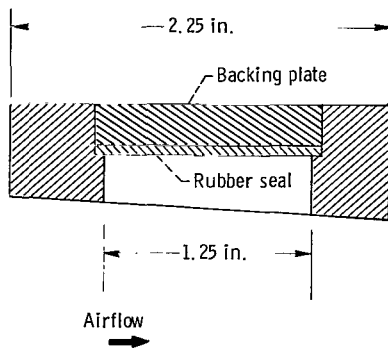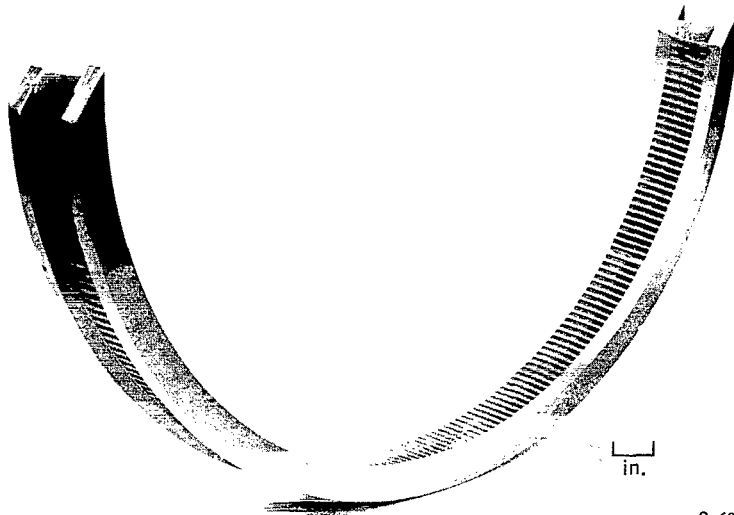
C-69-3794

Figure 8. – Skewed slotted casing insert.
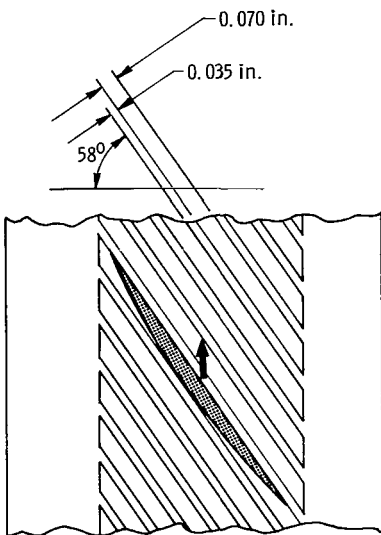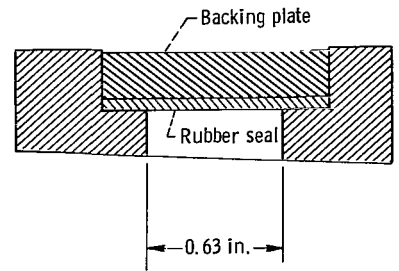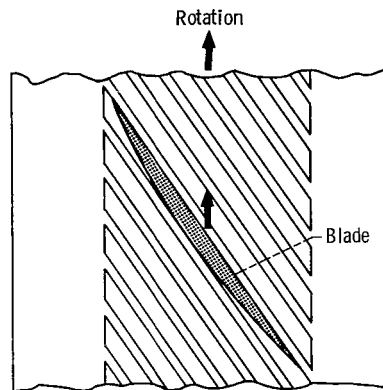
(a) Without rubber seal – open, deep, and long slots; and with rubber seal – closed, deep and long slots.

(b) Closed, shallow, and long slots.

(c) Closed, shallow, and short slots.

CD-11080-01

(d) Photograph of shallow, short slots.

C-70-647

Figure 9. - Blade angle slotted casing inserts.

urations and a photograph of the final configuration are shown in figure 9. The slots are alined with the average blade setting angle (58° to axial plane) of the blade tip section. Thus, a slot is affected by only one blade at a time. In the other slotted casings, a slot may be feeling the effect of several blades at a time. The slot width is twice the land width, and the open area is approximately two-thirds of the total area. There are 310 slots. Two radial depths were selected for testing, deep (average 0.64 in.; fig. 9(a)) and shallow (average 0.32 in.; figs. 9(b) and (c)). The deep slots were tested both with a rubber seal (closed slots) and without the rubber seal (open slots). Without the rubber seal, the deep slots are open to a small plenum (0.030 in. deep) and are tuned to blade passing frequency at 0.9 N_D. With the rubber seal, the tuned frequency is reduced by one half. The shallow slots were tested only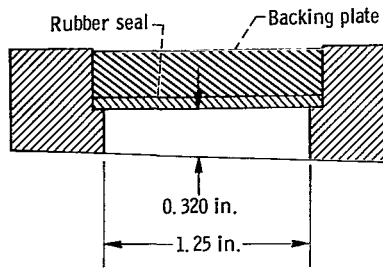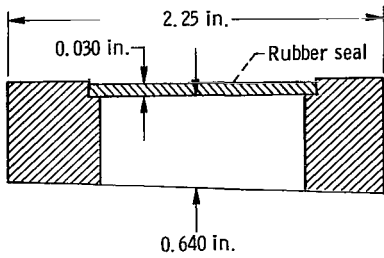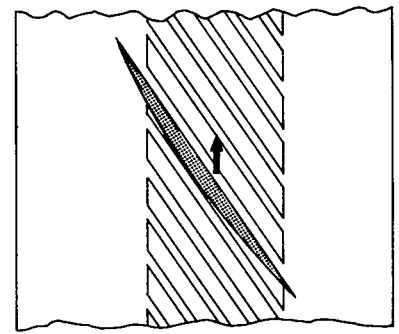 with a backing plate and rubber seal (closed slots), and the slots were tuned to blade passing frequency at 0.9 N_D. The configurations in which the slots extend beyond the leading and trailing edges of the rotor blades (fig. 9(a) and (b)) are called "long" slots. A modification to the shallow long slots consisted of cementing wood plugs in the slots at the upstream and downstream edges in order to shorten the slot length by 40 percent (in the axial plane). Thus, only the center section of the blade is subjected to casing treatment, and recirculation at the leading and trailing edges is minimized. This configuration is designated "shallow short," and a sketch is shown in figure 9(c) and a photograph in figure 9(d).

DISTORTION SCREENS

To generate both radial and circumferential inlet flow distortions, screens were mounted approximately 14 inches upstream of the rotor inlet (fig. 3). A schematic diagram of the two screens is presented in figure 10.

The 360° tip radial distortion screen (fig. 10(a)) was 20 mesh with 0.018-inch-diameter wire and extended into the flow stream a distance of 1.625 inches from the outer wall. This radial screen depth produced a loss in total pressure at the rotor inlet over approximately 40 percent of the blade height measured from the tip.

The circumferential screen (fig. 10(b)) was also 20 mesh with 0.018-inch-diameter wire. This screen covered a 90° segment of the inlet opening.

Both the radial and circumferential distortion screens were supported by a coarse screen having a 0.091-inch-diameter wire with 0.5-inch spacing.

1.625-in. fine mesh (20) radial screen

Fine mesh (20), 90° segment screen

Coarse mesh supporting screen

(a) Radial distortion screen.

(b) Circumferential distortion screen.
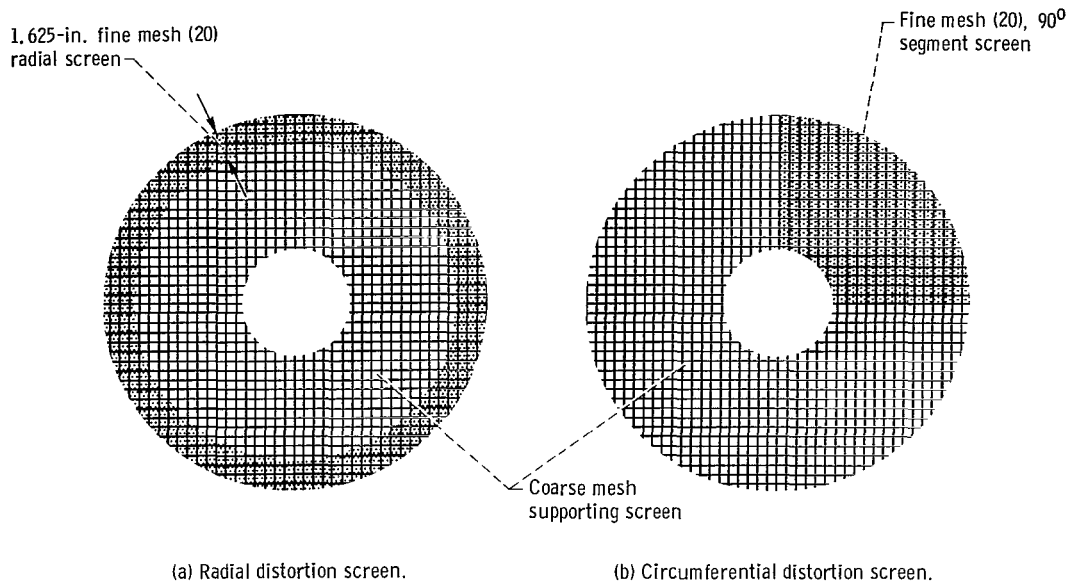
CD-11081-01

Figure 10. - Inlet flow distortion screens.

INSTRUMENTATION

Two iron-constantan thermocouples were located in the plenum tank for sensing plenum total temperature. Plenum total pressure was assumed equal to plenum static pressure and was determined from four manifolded wall static taps located approximately 90° apart on the plenum tank. The rotor outlet conditions were determined from measurements obtained from four rakes located approximately 90° apart and 11 inches downstream of the blade trailing edge (fig. 3). A photograph of one of the rakes is shown in figure 11. Each rake had five total-pressure elements located at 10, 30, 50, 70, and 90 percent of the passage height from the outer casing. Each rake also had five iron-constantan thermocouples located near the total-pressure elements. The rakes were positioned 45° from the axial direction. Outlet static pressure at the various rake positions was determined by assuming a linear variation between measured inner- and outer-wall static pressures. A hot-film anemometer probe located approximately 1 inch upstream of the blade-tip leading edge (fig. 3) was used for detecting the presence of rotating stall. Rotor speed was determined by the use of a magnetic pickup in conjunction with a gear mounted on the drive motor shaft. A calibrated orifice plate in the inlet line was used to determine the airflow rate. All data were measured by an automatic digital potentiometer and recorded on magnetic tape at a central recording area. An x-y plotter, which recorded the rotor discharge pressure and orifice ΔP (weight flow), was used for monitoring the tests.

16
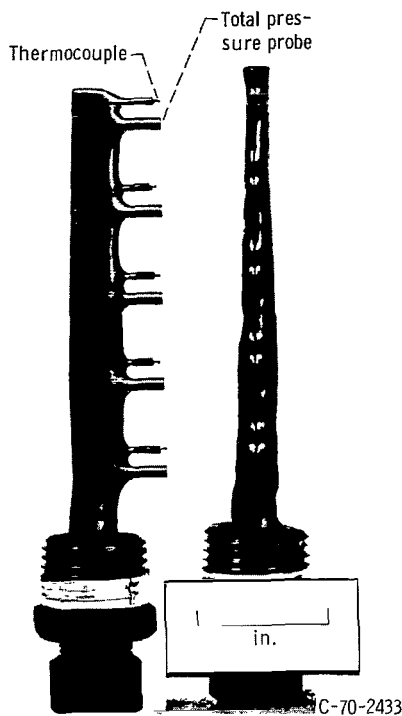
Figure 11. - Total-pressure - total-temperature rake.

The estimated errors of the data based on inherent accuracies of the instruments and recording systems are as follows:

Flow rate, lbm/sec . . . . ±0.5
Temperature, ^{O}R . . . . ±1.0
Inlet total pressure, psi . . . . ±0.05
Outlet wall static pressure, psi . . . . ±0.15
Outlet total pressure, psi . . . . ±0.15
Rotor speed, rpm . . . . ±50

TEST PROCEDURE

Data were recorded at 0.6, 0.7, 0.8, 0.9, and 1.0 of corrected design speed. The rotor data were taken over a range of weight flows from maximum flow to stall conditions at 0.7, 0.9, and 1.0 N_D. In general, it was attempted to define the operating curve by three points (maximum flow, midflow, and stall-limit flow). At 0.6 and 0.8 N_D, only the stall-limit points were taken in order to define the stall-limit line from 0.6 to 1.0 N_D.

17

The atmospheric air to the rotor inlet was not throttled (open inlet flow control valve) during this series of tests. An exhaust vacuum was used downstream of the outlet throttle valve to help overcome the losses in the discharge system.

The stall points were established by increasing the back pressure on the rotor (closing outlet flow control valve) until a rapid signal fluctuation was noted from the hot-wire anemometer probe. This was generally accompanied by a drop in outlet pressure and an increase in audible noise level. The data stall point was then set near the actual stall point recorded on the x-y plotter.

PERFORMANCE CALCULATION PROCEDURE

The overall rotor performance is based on average conditions in the plenum tank and arithmetically averaged values of temperature and pressure at the rotor outlet as determined by the outlet rake instrumentation. Outlet temperature measurements were corrected for Mach number. All performance parameters were corrected to standard day conditions based on plenum measurements.

The percent stall margin increase (at a given speed) that might be obtained with casing treatment as compared with that with no casing treatment was determined from the following formula:

percent stall margin over solid-wall reference

$$
= \left[\frac{(\text{pressure ratio})_{\text{casing treatment stall point}}}{(\text{pressure ratio})_{\text{reference stall point}}} \times \frac{\left(\frac{W\sqrt{\theta}}{\delta}\right)_{\text{reference stall point}}}{\left(\frac{W\sqrt{\theta}}{\delta}\right)_{\text{casing treatment stall point}}} - 1 \right] 100
$$

This is not the normal usage of the term stall margin. It is usually based on the pressure-ratio and weight flow from a chosen operating point and the stall point on a constant-speed - performance curve (ref. 3).

The weight flows obtained with uniform inlet flow cannot be compared with those obtained with nonuniform inlet flow because the data were corrected to plenum conditions and thus do not include the losses due to the distortion screen. Also, the absolute rotor efficiencies obtained with nonuniform inlet flow are low as they include the total pressure loss across the screen. However, they may be used for comparing the effectiveness of the casing treatments with similar inlet flow distortions.

18

RESULTS AND DISCUSSION

Several geometrically different casing treatments were evaluated for their ability to improve the rotor performance. The effectiveness of the casing treatments investigated are judged primarily by their ability to move the rotor stall-limit line to lower weight flows than the reference stall-limit line obtained with a solid casing. The overall rotor performances shown herein are based on data obtained from downstream rake instrumentation in which the individual parameters are arithmetically averaged.

The results of this investigation are presented in three main sections: (1) rotor performance with reference solid casing (no treatment) (2) rotor performance with casing treatments, and (3) comparison of stall-limit lines.

The rotor performance is presented for uniform inlet-flow conditions for the reference casing and all the casing treatment configurations. The rotor performance is also presented for tip radially distorted inlet flow for the reference casing and, in general, for those casing treatments that showed a substantial improvement in performance with uniform inlet-flow conditions. Two of the casing treatment configurations were also tested with circumferentially distorted inlet flow.

ROTOR PERFORMANCE WITH SOLID (REFERENCE) CASING

The overall rotor performance for the reference solid casing is presented in figure 12 for uniform inlet flow and for radially distorted inlet flow. Total pressure ratio, total temperature ratio, and temperature rise are presented as functions of equivalent weight flow for speeds from 0.6 to 1.0 N_D.

Uniform Inlet Flow

At design speed, the stall-limit point occurred at a pressure ratio of 1.765 and a weight flow of 63.46 pounds per second (fig. 12(a)). This point will be used as the reference stall-limit point in determining stall-margin increases with casing treatment at design speed for uniform inlet flow. Maximum efficiency of 0.841 was obtained near the stall-limit point at a weight flow of 63.80 pounds per second. Very little flow range is indicated (65.70 to 63.46 lbm/sec). The stall-limit line shown on the performance map from 0.6 to 1.0 N_D will hereafter be referred to as the "reference stall-limit line" for uniform inlet flow conditions.
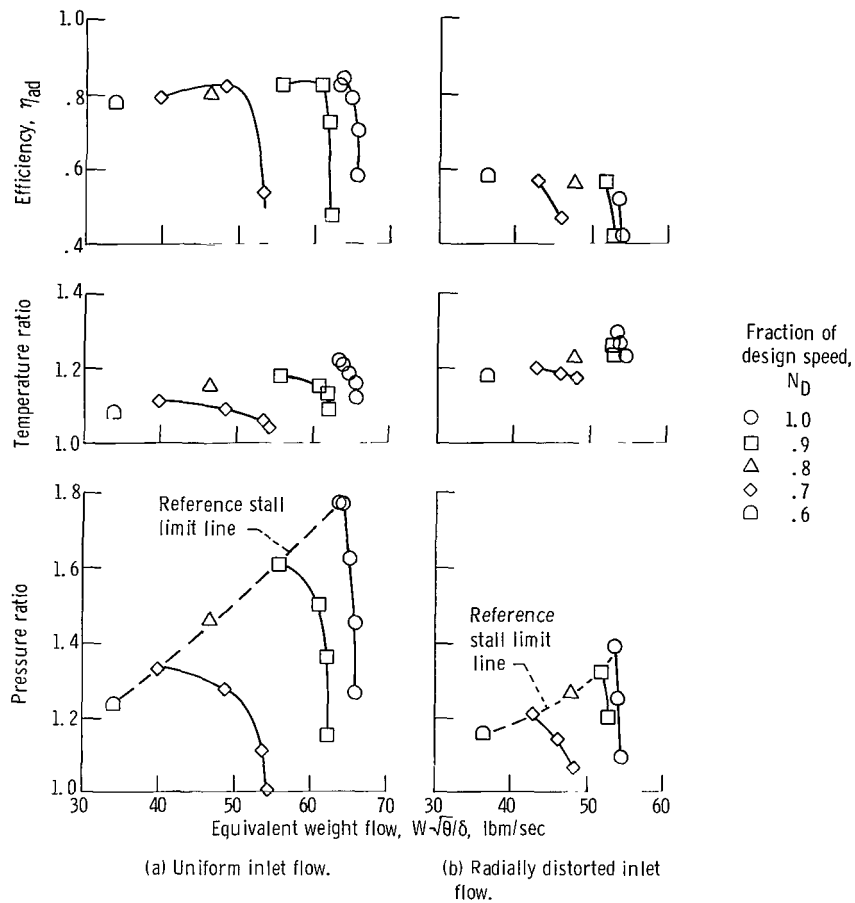
Figure 12. - Overall rotor performance with solid casing insert (reference).

Radially Distorted Inlet Flow

At design speed, the stall-limit point occurred at a pressure ratio of 1.392 and a weight flow of 53.49 pounds per second (fig. 12(b)). A maximum efficiency of 0.512 was also obtained at the stall point. This point will be used as the reference stall-limit point in determining stall-margin increases with casing treatment at design speed for radially distorted inlet flow. Very little flow range is indicated at design speed (54.55 to 53.49 lbm/sec). The stall-limit line shown on the performance map from 0.6 to 1.0 N_D will hereinafter be referred to as the reference stall-limit line for radially distorted inlet flow.

As pointed out in the calculation procedure section, comparisons cannot be made for the same configuration with uniform inlet flow and radially distorted inlet flow. Also, the efficiencies for radially distorted inlet flow are low, but they can be used for comparison purposes.

20

ROTOR PERFORMANCE WITH CASING TREATMENT

The overall rotor performances presented in this section will be shown in terms of total pressure ratio, total temperature ratio, and temperature-rise efficiency as a function of equivalent weight flow. Where applicable, the stall-margin increase (see calculation procedure) obtained with casing treatment will be given for $1.0 \ N_D$. The stall limit line from 0.6 to $1.0 \ N_D$ will be shown along with the reference stall-limit line.

Perforated Casing with Small Holes

The overall rotor performance for the perforated casing with small holes (0.0625-in. diam) is presented in figure 13 for uniform inlet flow. At design speed, the stall-limit point occurred at a pressure ratio of 1.754 and a weight flow of 62.96 pounds per second. A maximum efficiency of 0.839 was also obtained at the stall point. No stall
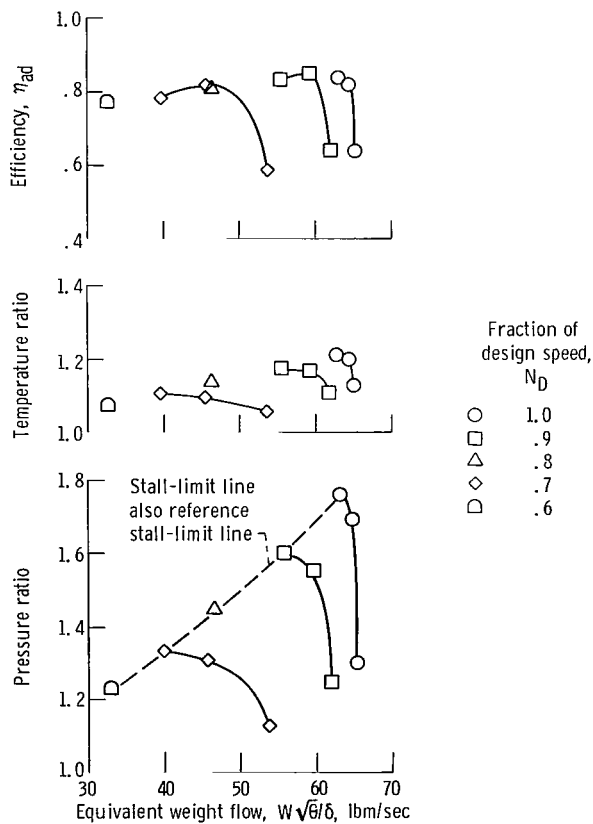
Figure 13. - Overall rotor performance for perforated casing with 0.0625-inch-diameter holes; uniform inlet flow.

margin increase over the reference casing was obtained. This casing treatment has essentially the same stall-limit line as that of the reference solid casing. In general, the overall performance is nearly the same as for the solid casing. Thus, this casing treatment was not tested with radially distorted inlet flow.

Perforated Casing with Large Holes

The overall rotor performance with a perforated casing with large holes (0. 125-in. diam) is presented in figure 14 for uniform inlet flow. At design speed, the stall-limit point occurred at a pressure ratio of 1.760 and a weight flow of 62.48 pounds per second. A maximum efficiency of 0.820 was also obtained at the stall point. The stall-margin increase over the reference casing was approximately 1.3 percent. A comparison of the stall-limit lines shows a small displacement of the stall-limit line from the reference line to lower weight flows at low speeds but very little displacement at high speeds. It appears that the greater open area of the perforated casing with large holes is more beneficial than the one with small holes. However, the performance improvement was not
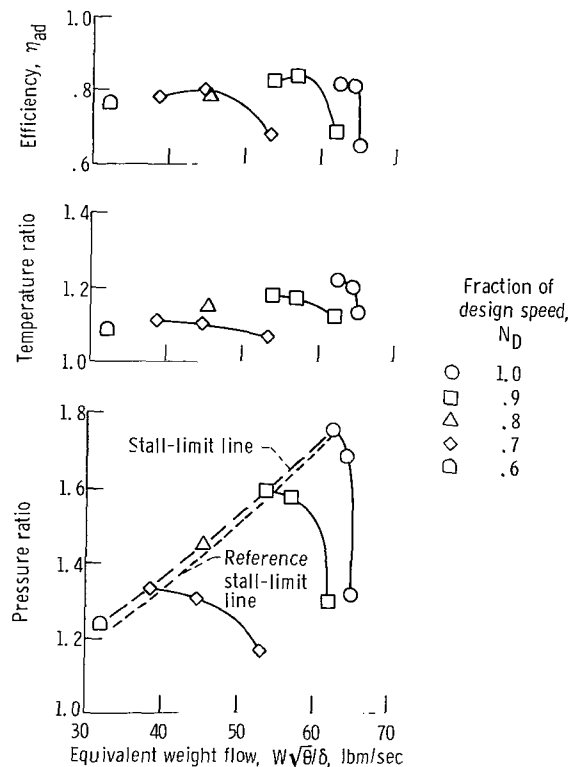
Figure 14. - Overall rotor performance for perforated casing with 0. 125-inch-diameter holes; uniform inlet flow.

considered large enough to justify testing this configuration with radially distorted inlet flow.

Honeycomb Casing with Deep, Small Cells

The overall rotor performance with a honeycomb casing with deep (average, 0.55 in.) and small cells (0.19 by 0.11 in.) is presented in figure 15(a) for uniform inlet flow and figure 15(b) for radially distorted inlet flow.

Uniform inlet flow. - At design speed, the stall-limit point occurred at a pressure ratio of 1.792 and a weight flow of 57.49 pounds per second (fig. 15(a)). The stall-margin increase over the reference casing was approximately 12 percent. A maximum efficiency of 0.817 was obtained at a weight flow of 63.71 pounds per second. This is approximately 2.5 percentage points lower than the maximum efficiency for the reference casing. There is a good displacement of the stall-limit line from the reference line to

(a) Uniform inlet flow. (b) Radially distorted inlet flow.
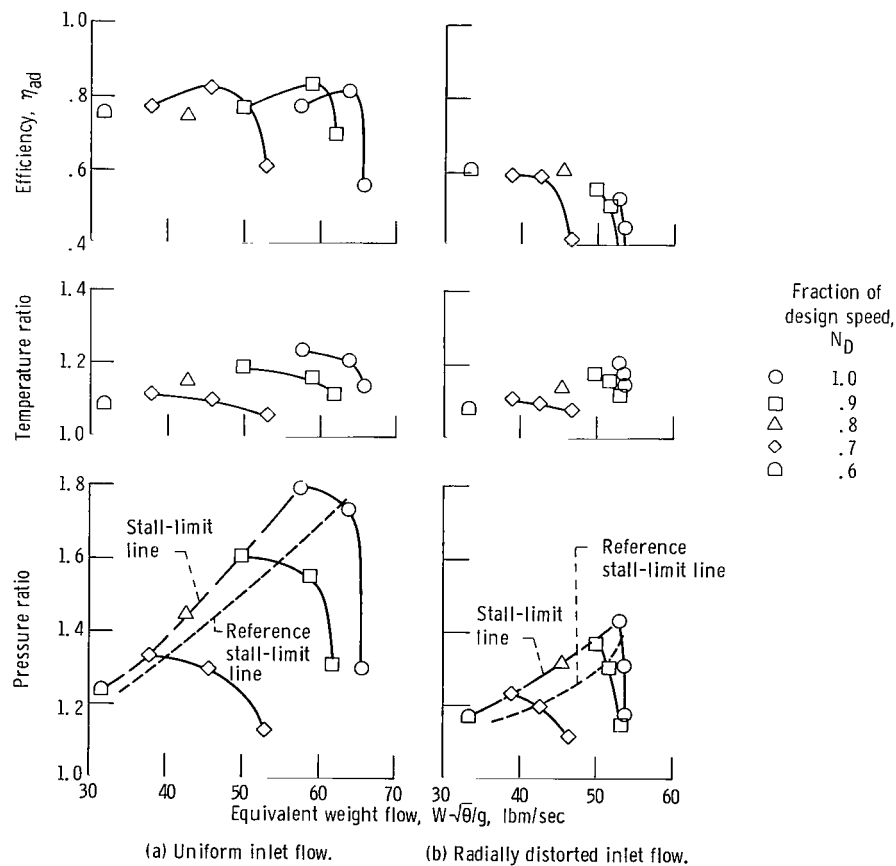
Figure 15. - Overall rotor performance for honeycomb casing with deep and small (0.19 by 0.11 in.) cells.

lower weight flows, particularly at the higher speeds. Slight damage of the soft alumi-
num honeycomb cells over the rotor tip was observed after the tests.

Radially distorted inlet flow. - At design speed, the stall-limit point occurred at a
pressure ratio of 1.431 and a weight flow of 52.94 pounds per second (fig. 15(b)). A
maximum efficiency of 0.528 was also obtained at the stall point. The stall margin in-
crease over the reference casing was approximately 3.9 percent. It appears that the
maximum efficiency at all speeds occurs at the stall point as it also did for the reference
casing with radial distortion. The maximum efficiencies are low (0.52 to 0.61) and re-
flect the losses due to the distortion screen but are a few percentage points higher than
those obtained with the reference casing. There has been a displacement of the stall-
limit line from the reference line to lower weight flows, but the displacement is not large
at 1.0 N_D. Additional honeycomb deterioration was observed after the radial distortion
tests.

Honeycomb Casing with Shallow, Small Cells

The overall rotor performance with a honeycomb casing with shallow (average 0.32
in.) and small cells (0.19 by 0.11 in.) is presented in figure 16 for uniform inlet flow.
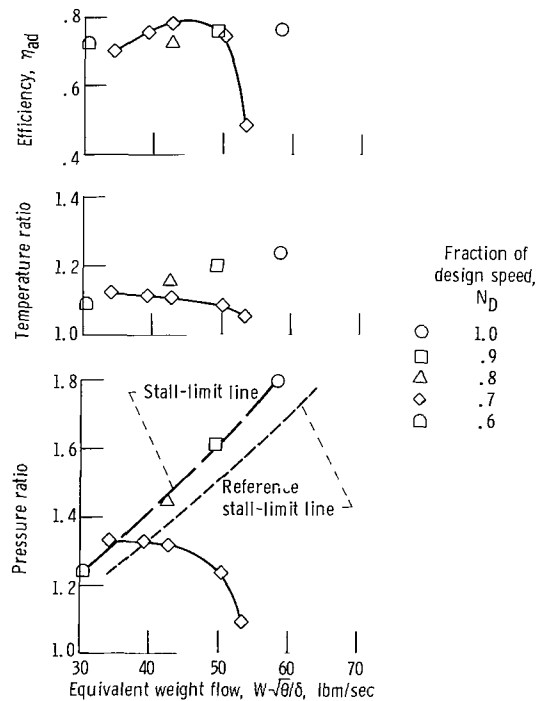
Figure 16. - Overall rotor performance for honeycomb casing
with shallow and small (0.19 by 0.11 in.) cells; uniform
inlet flow.

24

At design speed, the stall-limit point occurred at a pressure ratio of 1.797 and a weight flow of 58.43 pounds per second. The efficiency was 0.767. The stall-margin increase over the reference casing was approximately 11 percent. Except at 0.7 N_D, only stall-point data were taken in order to limit the test time and to prevent deterioration of the soft aluminum cells. There has been a displacement of the stall-limit line from the reference line to lower weight flows. However, the displacement is about the same as that obtained with the deep, small-cell honeycomb at speeds above 0.8 N_D. Therefore, this configuration was not tested with inlet radial distortion. This configuration is one in which the cell depth was chosen for resonance with blade passing frequency at 0.9 N_D. It appears that tuning neither benefits nor detracts from the rotor performance with the honeycomb casings.

Honeycomb Casing with Deep, Large Cells

The overall rotor performance with a honeycomb casing with deep (average 0.55 in.)
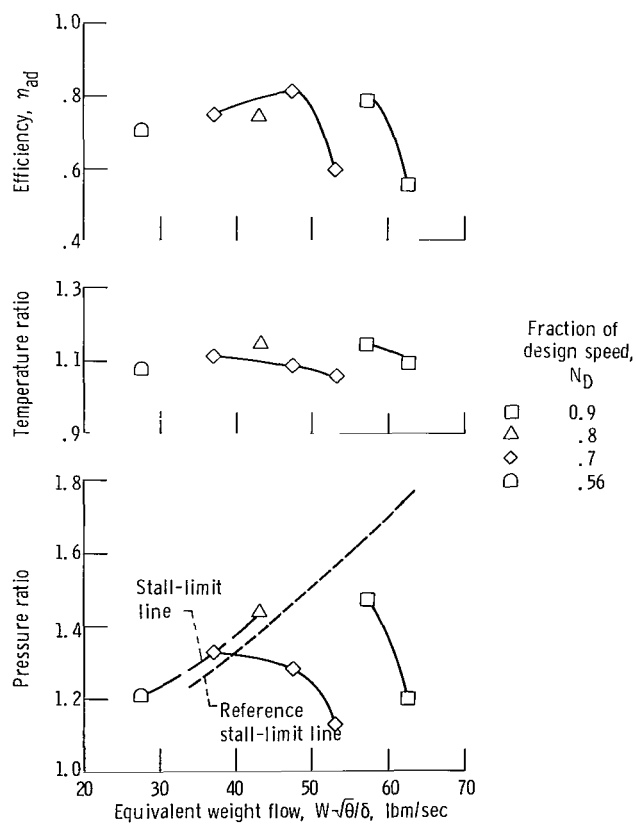
Figure 17. - Overall rotor performance for honeycomb casing with deep and large (0.33 by 0.20 in.) cell; uniform inlet flow.

and large cells (0. 33 by 0. 20 in.) is presented in figure 17 for uniform inlet flow. During the tests there was a rapid deterioration of the large-cell structure above the rotor (fig. 18) and data are shown only to 0.9 N_D. The stall-limit point at 0.9 N_D could not be obtained. The performance curve at 0.7 N_D was completed, and a maximum efficiency of 0.809 was obtained. This is approximately the same as that obtained with the other two honeycomb configurations at 0.7 N_D. A section of the stall-limit line is shown between 0.6 N_D and 0.8 N_D, and it appears that the displacement from the reference line to lower weight flows is about the same as the other honeycomb configurations. Because of the cell deterioration, the large-cell honeycomb was not tested with radial distortion at inlet.

1 in.   C-69-3799
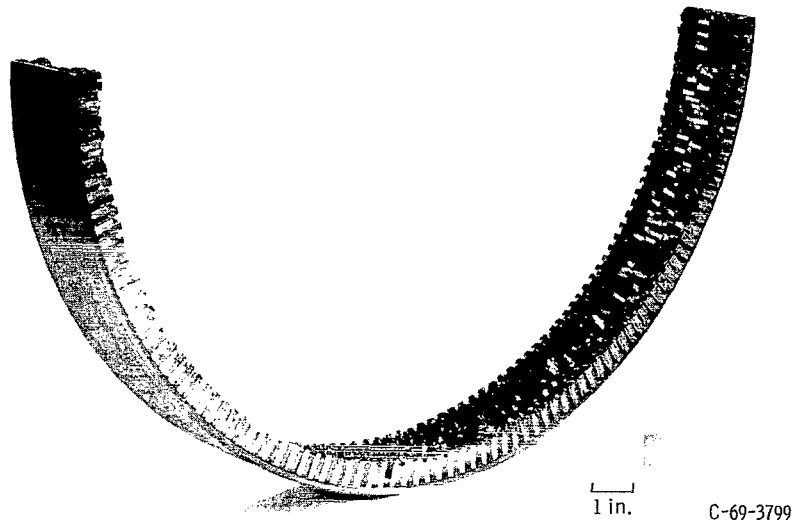
Figure 18. – Damaged honeycomb casing with deep and large cells.

Circumferentially Grooved Casing

The overall rotor performance with a circumferentially grooved casing is presented in figure 19(a) for uniform inlet flow and in figure 19(b) for radially distorted inlet flow.

Uniform inlet flow. - At design speed, the stall-limit point occurred at a pressure ratio of 1.833 and a weight flow of 58.09 pounds per second. The stall-margin increase over the reference casing was approximately 13.5 percent. The maximum efficiency was 0.858 at a weight flow of 61.58 pounds per second and was nearly constant to a weight flow of 64.75 pounds per second. The maximum efficiency was approximately 1.5 percentage points higher than that obtained with the reference solid casing. At the higher

26
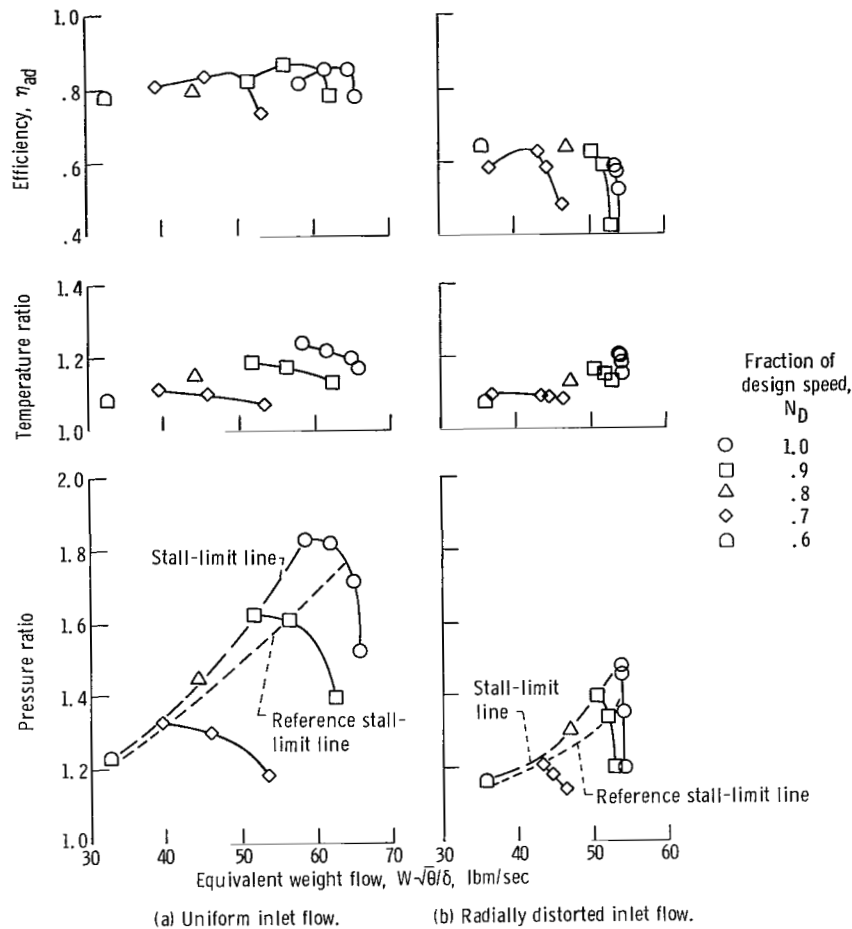
Figure 19. - Overall rotor performance for circumferentially grooved casing.

speeds, the circumferentially grooved casing gives a good displacement of the stall-limit line from the reference line to lower weight flows. At speeds of $0.7 N_D$ and lower there is only a small displacement of the stall-limit line. In general, this casing treatment gives improved high speed performance. It is easily fabricated, and might readily be incorporated in a production type casing.

Radially distorted inlet flow. - At design speed, the stall-limit point occurred at a pressure ratio of 1.473 and a weight flow of 53.45 pounds per second (fig. 19(b)). A maximum efficiency of 0.583 was also obtained at the stall point. The stall-margin increase over the reference casing was approximately 5.9 percent. Maximum efficiencies at all speeds appear to be 5 to 8 percentage points higher than those obtained with the reference casing. There is a good displacement of the stall-limit line from the reference line to lower weight flows at speeds above $0.8 N_D$.

Axially Slotted Casing

The overall rotor performance with an axially slotted casing is presented in figure 20 for uniform inlet flow. For this configuration, recirculation of air is possible between slots and also from the slots into the main flow stream ahead of the blade-tip leading edge. The slots are tuned to blade passing frequency at $0.9 \ N_D$. Post-test examination of the casing insert revealed considerable damage to the slots (see fig. 21). The damage was probably due to thermal expansion of the aluminum insert against the steel casing, which caused the thin walls of the slots to collapse. At design speed, there was a loss in rotor performance with the stall-limit point falling on the reference stall-limit line but at
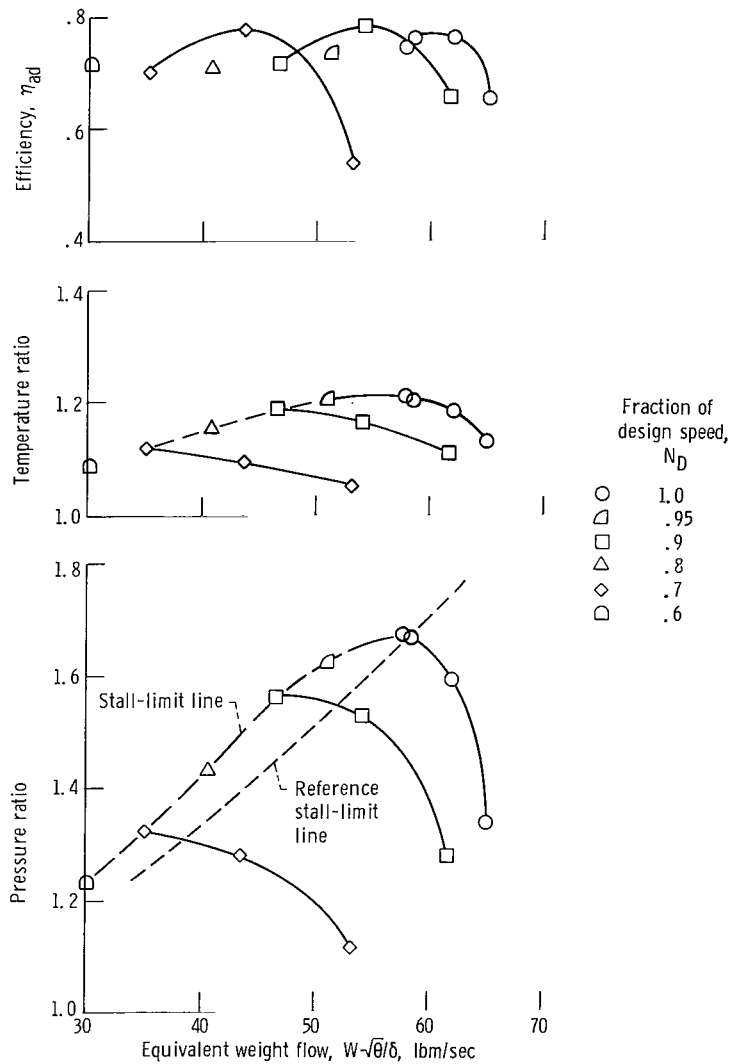
Figure 20. - Overall rotor performance for axially slotted casing; uniform inlet flow.
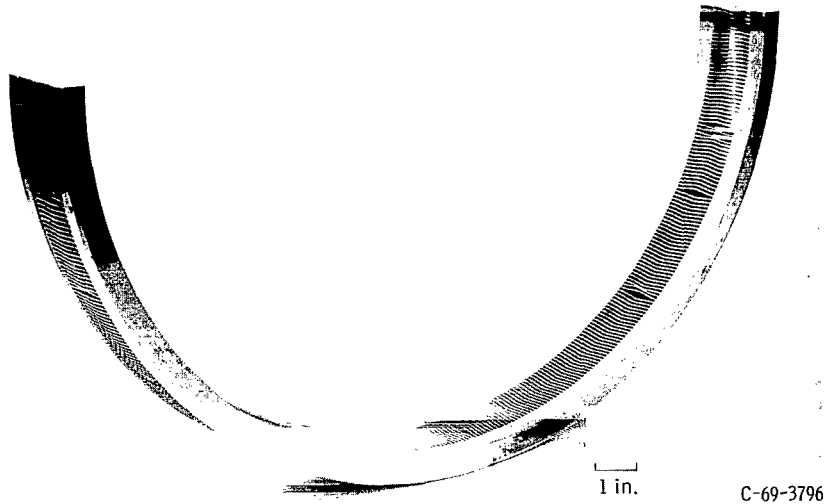
Figure 21. - Damaged axially slotted casing.

a much lower pressure ratio than that for the reference solid casing. It is possible that the damage to the slots during the tests contributed to the rotor's poor performance at design speed. However, there is a good displacement of the stall-limit line from the reference lines to lower weight flows at speeds below 0.95 N_D. At 0.9 N_D the stall-margin increase over the reference casing was approximately 15.8 percent. The maximum efficiencies were approximately 6 percentage points lower than those obtained for the reference solid casing.

Skewed Slotted Casing with Slots Open to Chamber

The overall rotor performance with a skewed slotted casing with open slots is presented in figure 22(a) for uniform inlet flow and in figure 22(b) for radially distorted inlet flow. For this configuration, recirculation of air is possible between slots and also from the slots into the main flow stream ahead of the blade tip leading edge. The slots are tuned to blade passing frequency at 0.9 N_D.

Uniform inlet flow. - At design speed, the stall-limit point occurred at a pressure ratio of 1.824 and a weight flow of 54.35 pounds per second (fig. 22(a)). The stall-margin increase over the reference casing was approximately 20.7 percent. The maximum efficiency was 0.771 at a weight flow of 62.58 pounds per second. This is approximately 7 percentage points lower than that obtained with the reference casing. However, at 0.7 and 0.9 N_D, the maximum efficiencies were only 2 percentage points lower.

29
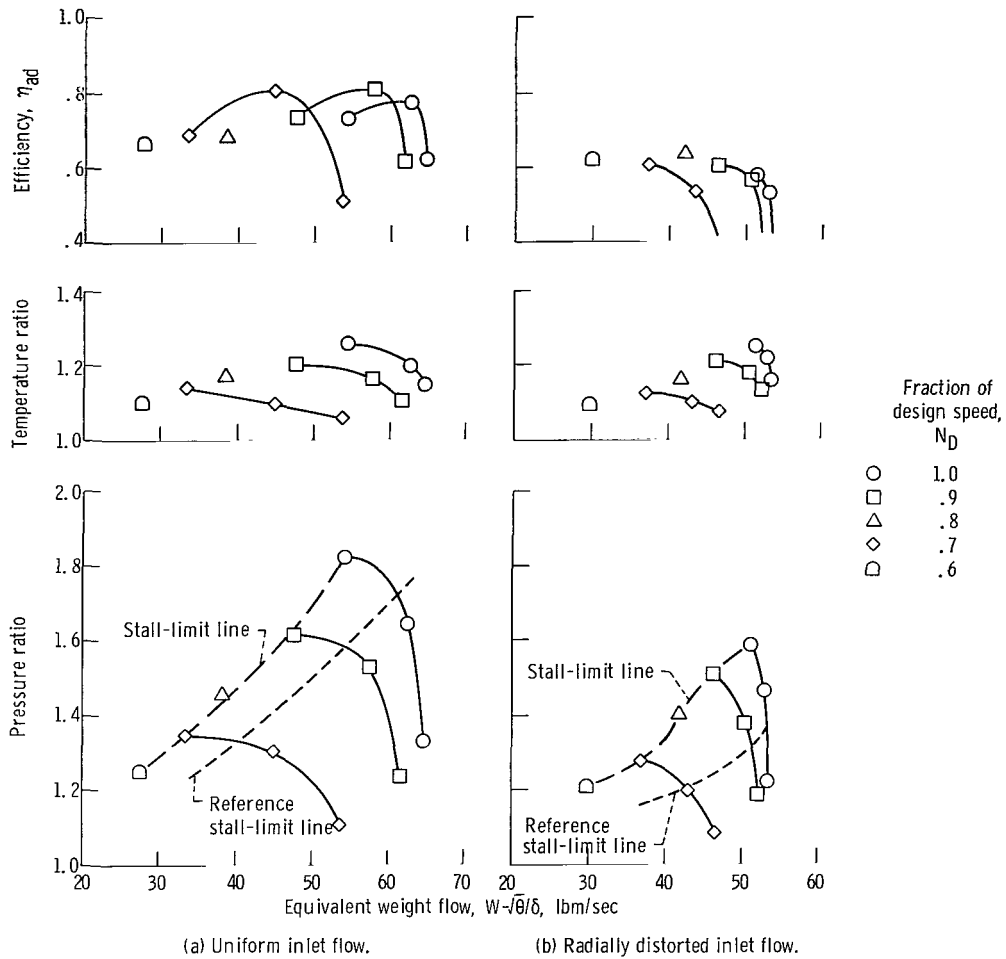
Figure 22. - Overall rotor performance for skewed slotted casing with slots open to chamber.

There has been a very good displacement of the stall-limit line from the reference line to lower weight flows at all speeds.

Radially distorted inlet flow. - At design speed, the stall-limit point occurred at a pressure ratio of 1.588 and a weight flow of 51.24 pounds per second (fig. 22(b)). A maximum efficiency of 0.576 was also obtained at the stall point. The stall-margin increase over the reference casing was approximately 19.1 percent. Maximum efficiencies at all speeds are 4 to 8 percentage points higher than those obtained with the reference casing. There has been a very large displacement of the stall-limit line from the reference line to lower weight flows and high pressure ratios at all speeds.

Skewed Slotted Casing with Closed Slots

The overall rotor performance with a skewed slotted casing with closed slots is presented in figure 23 for uniform flow and for radially distorted inlet flow. For this configuration, recirculation of air between slots is prevented by closing the slots, but recirculation of air is possible from the slot into the main flow stream ahead of the blade-tip leading edge. The slots are tuned to blade passing frequency at 0.45 N_D (one-half that of the open slots).

Uniform inlet flow. - At design speed, the stall-limit point occurred at a pressure ratio of 1.809 and a weight flow of 56.42 pounds per second (fig. 23(a)). The stall-
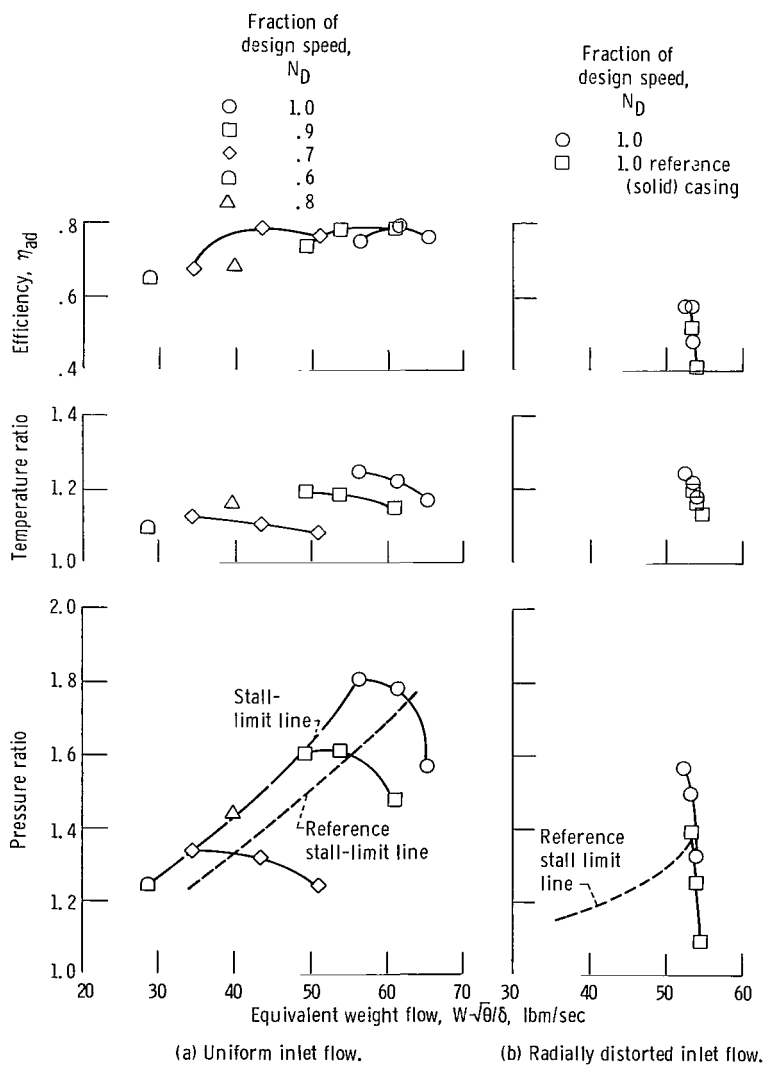

Figure 23. - Overall rotor performance for skewed slotted casing with closed slots.

(a) Uniform inlet flow.   (b) Radially distorted inlet flow.

margin increase over the reference casing was approximately 15.3 percent. A maximum efficiency of 0.793 was obtained at a weight flow of 61.34 pounds per second. The maximum efficiencies over the speed range are about 5 percentage points lower than those obtained with the reference solid casing. There is a good displacement of the stall-limit line from the reference line to lower weight flows. The stall-margin increase was less (5 percent at 1.0 N_D) than that obtained with the skewed open slots.

Radially distorted inlet flow. - At design speed, the stall-limit point occurred at a pressure ratio of 1.568 and a weight flow of 52.38 pounds per second. A maximum efficiency of 0.571 was also obtained at the stall point. The stall-margin increase over the reference casing was approximately 15 percent. This is approximately 4 percentage points lower than the stall-margin increase obtained with skewed open slots with radially distorted inlet flow. Only design speed performance was obtained for this configuration. However, it appears that a good displacement of the stall-limit line from the reference line to lower flows and higher pressure ratios might be obtained with the skewed, closed slots.

Blade Angle Slotted Casing with Deep, Long Slots Open to Chamber

The overall rotor performance with a blade angle slotted casing with open, deep, and long slots is presented in figure 24 for uniform inlet flow and for radially distorted inlet flow. For this configuration, recirculation of air is possible between slots and, also, from the slots into the main flow stream ahead of the blade-tip leading edge. The slots are tuned to blade passing frequency at 0.9 N_D.

Uniform inlet flow. - At design speed, the stall-limit point occurred at a pressure ratio of 1.602 and a weight flow of 56.77 pounds per second (fig. 24(a)). A maximum efficiency of 0.759 was obtained at a weight flow of 60.46 pounds per second. A stall-margin increase of 1.5 percent over the reference casing was obtained. However, care must be taken in interpreting the increase in stall margin as it results only from a large decrease in the stall weight flow. The stall pressure ratio was considerably lower than that for the reference casing, and approximately the same performance with a higher efficiency could be obtained with the reference casing with the rotor operating at a lower speed. The stall-limit line moved to the right of or to higher weight flows than the reference stall-limit line. In general, the rotor performance deteriorated with this casing treatment.

Radially distorted inlet flow. - At design speed, a pressure ratio of approximately 1.40 was obtained over a relatively large flow range (fig. 24(b)). No stall-limit point could be found. But the increase in stall margin over the reference casing for the lowest weight-flow point shown was approximately 140 percent. The maximum efficiency was
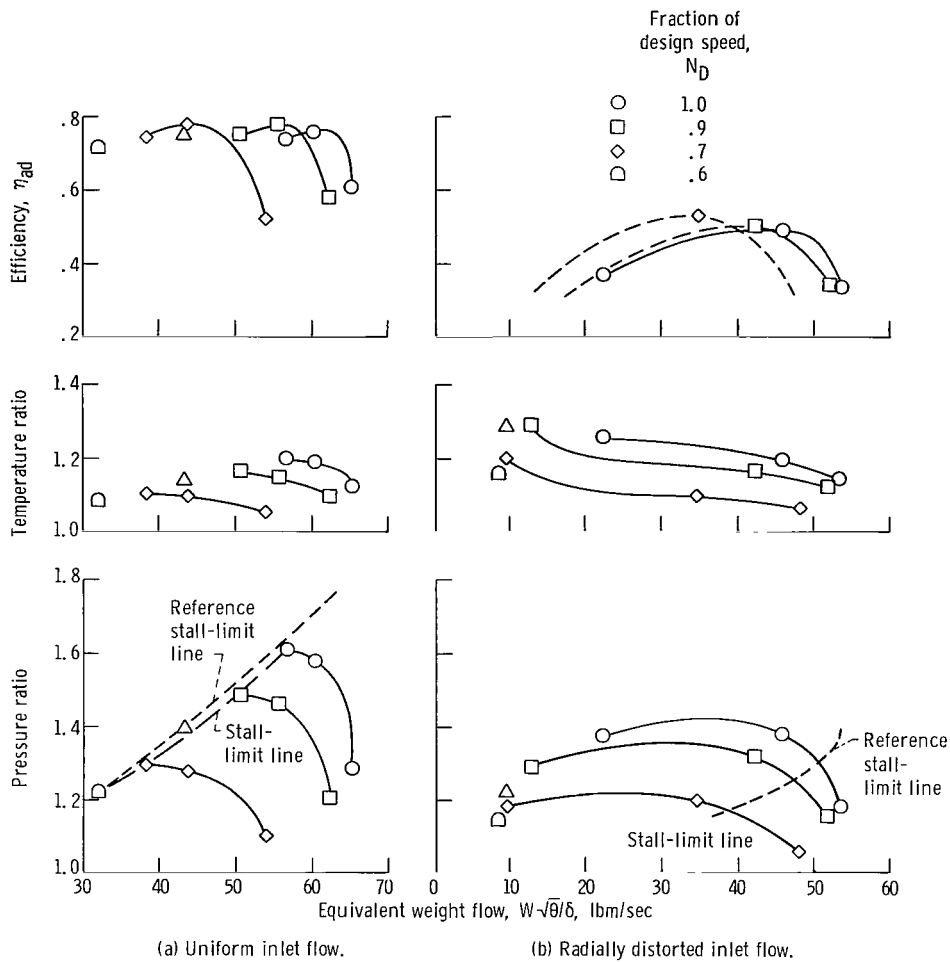
Figure 24. - Overall rotor performance for blade angle slotted casing with deep and long slots open to chamber.

approximately 0.49, which is about 2 percentage points lower than that obtained for the reference solid casing. No stall-limit line is shown because stall points could not be determined at any speed. Although the rotor performance with this casing treatment was poor with uniform inlet flow, the treatment enabled the rotor to become extremely tolerant of radially distorted inlet flow.

Blade Angle Slotted Casing with Closed, Deep, and Long Slots

The overall rotor performance with a blade angle slotted casing with closed, deep, and long slots is presented in figure 25 for uniform inlet flow and for radially distorted inlet flow. For this configuration, recirculation of air between slots is prevented by

Figure 25. - Overall rotor performance for blade angle slotted casing with closed, deep, and long slots.

closing the slots. Recirculation of air is possible from the slot into the main flow stream ahead of the blade-tip leading edge as the slots extend beyond the blade-tip leading edge. The slots are tuned to blade passing frequency at 0.45 N_D (one-half that of the blade angle casing with open slots).

Uniform inlet flow. - At design speed, the stall-limit point occurred at a pressure ratio of 1.598 and a weight flow of 56.20 pounds per second (fig. 25(a)). Although the stall weight flow is lower than the reference stall weight flow, the increase in stall margin over the reference casing was small (2.2 percent) because of the much lower pressure ratio. A maximum efficiency of 0.774 was obtained at a weight flow of 58.64 pounds per second. The stall-limit line shifted slightly to the right (to higher weight flows) of the reference stall-limit line. The performance is about the same as it was for the open-slot configuration. Thus, preventing recirculation of air between slots and changing the tuning frequency by one-half appears to have had little or no effect on the rotor performance.

Radially distorted inlet flow. - At design speed, the stall-limit point occurred at a pressure ratio of 1.382 and a weight flow of 34.77 pounds per second (fig. 25(b)). The stall-margin increase over the reference casing was approximately 52.8 percent. A

maximum efficiency of 0.512 was obtained at a weight flow of 46.58 pounds per second. This efficiency is about the same as that obtained for the reference solid casing. There is a large displacement of the stall-limit line from the reference line to lower weight flows. As in the case of the blade-angle-open slots, the closed slots enabled the rotor to be very tolerant of radially distorted inlet flow. However, a definite stall-limit point was obtained with the closed slots.

Blade Angle Slotted Casing with Closed, Shallow, and Long Slots

The overall rotor performance with a blade angle slotted casing with closed, shallow, and long slots is presented in figure 26 for uniform inlet flow and for radially distorted inlet flow. For this configuration, recircula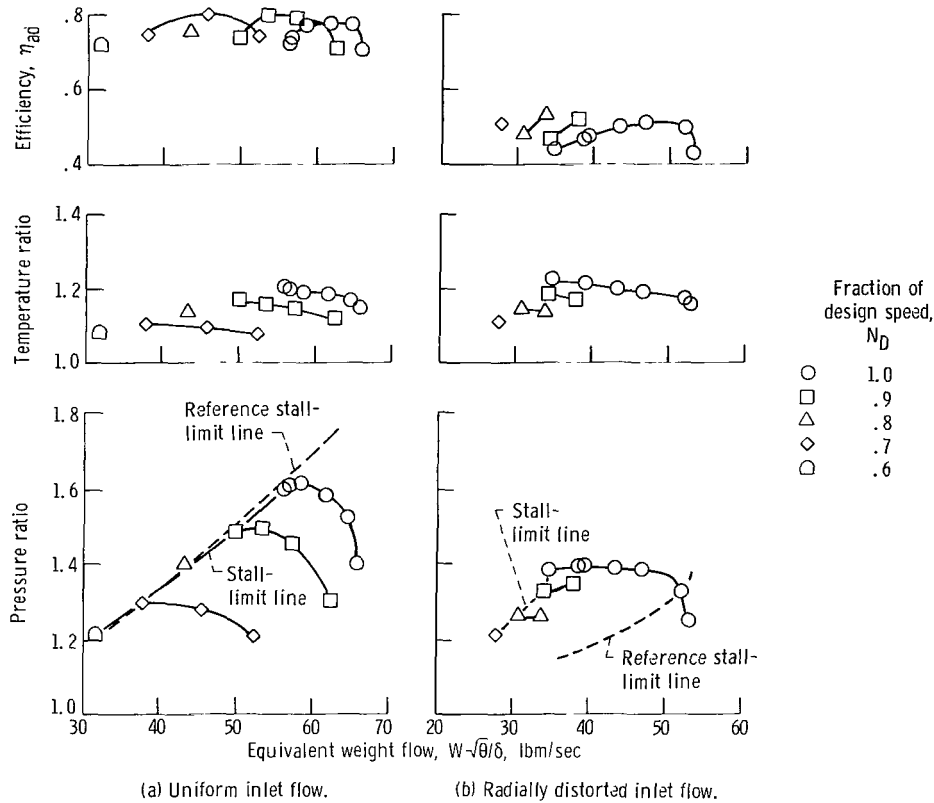tion of air between slots was prevented by closing the slots. Recirculation of air is possible from the slot into the main flow stream ahead of the blade-tip leading edge as the slots extend beyond the blade-tip leading edge. Although the slot depth has been changed by a factor of one-half from deep to shallow, closing the back of the slots keeps the slots tuned to blade passing frequency at 0.9 N_D.
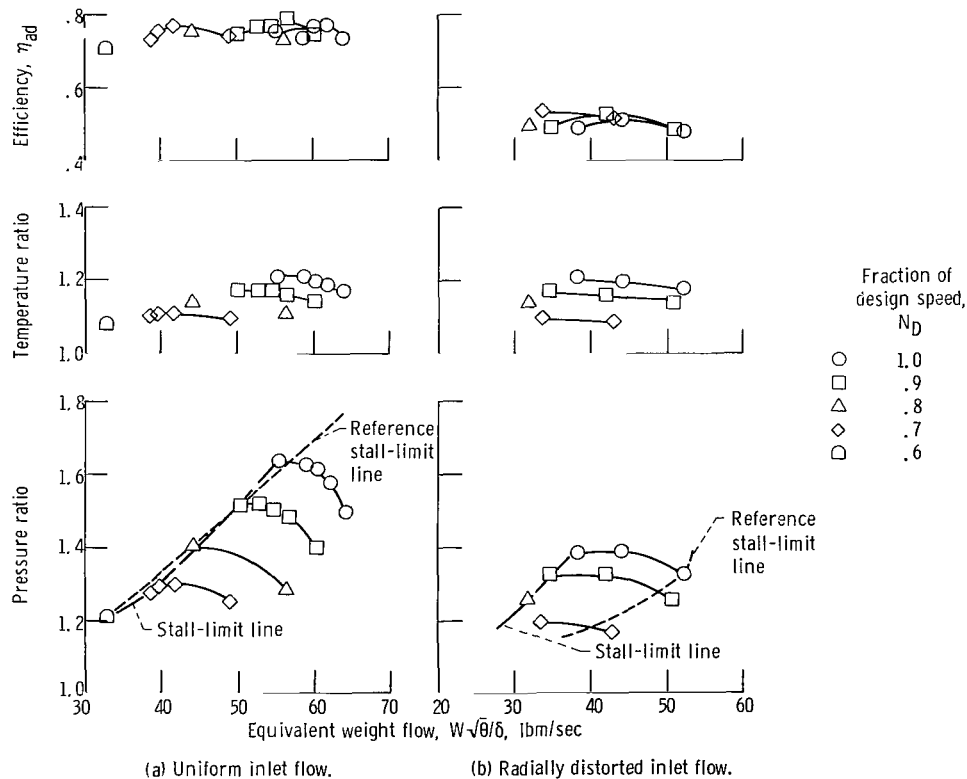

Figure 26. - Overall rotor performance for blade angle slotted casing with closed, shallow, and long slots.

Uniform inlet flow. - At design speed, the stall-limit point occurred at a pressure ratio of 1.633 and a weight flow of 55.18 pounds per second (fig. 26(a)). The stall-margin increase over the reference casing was approximately 6.5 percent. However, care must be taken in interpreting this increase in stall margin, as it has been obtained from a large reduction in weight flow. The combination of lower weight flow and lower pressure ratio causes the stall-limit point to fall close to the reference stall-limit line. Thus, nearly the same performance with a higher efficiency could be obtained from the reference casing with the rotor operating at a lower speed. A maximum efficiency (at 1.0 N_D) of 0.769 was obtained at a weight flow of 61.96 pounds per second. This efficiency is approximately 7 percentage points lower than that obtained for the reference solid casing. The stall-limit line is in approximately the same location as the reference stall-limit line except that it does not extend to as high a pressure ratio.

Radially distorted inlet flow. - At design speed, the stall-limit point occurred at a pressure ratio of 1.386 and a weight flow of 38.15 pounds per second. The stall margin increase over the reference casing was approximately 39.7 percent. A maximum efficiency of 0.508 was obtained at a weight flow of 44.11 pounds per second. This efficiency is about the same as that obtained for the reference casing. There is a good displacement of the stall-limit line from the reference line to lower weight flows. However, the displacement was not as great as it was for either of the deep blade angle configurations.

Blade Angle Slotted Casing with Closed, Shallow, and Short Slots

The overall rotor performance with a blade angle slotted casing with closed, shallow, and short slots is presented in figure 27 for uniform inlet flow and for radially distorted inlet flow. For this configuration, recirculation of air between slots was prevented by closing the slots. Recirculation of air from the slot into the main flow stream ahead of the rotor was also prevented by shortening the slots so that the casing treatment extended only over the center portion of the blade tip. The closed, shallow slots were tuned to blade passing frequency at 0.9 N_D.

Uniform inlet flow. - At design speed, the stall-limit point occurred at a pressure ratio of 1.827 and a weight flow of 55.89 pounds per second (fig. 27(a)). The stall-margin increase over the reference casing was approximately 17.5 percent. For this configuration, a reduction in weight flow and an increase in pressure-ratio was obtained at the stall-limit point as compared with the reference stall-limit point. A maximum efficiency of 0.847 was obtained at a weight flow of 63.75 pounds per second. This efficiency is as high as or slightly higher than that obtained with the reference casing. There is a marked displacement of the stall-limit line from the reference line to lower weight flows.
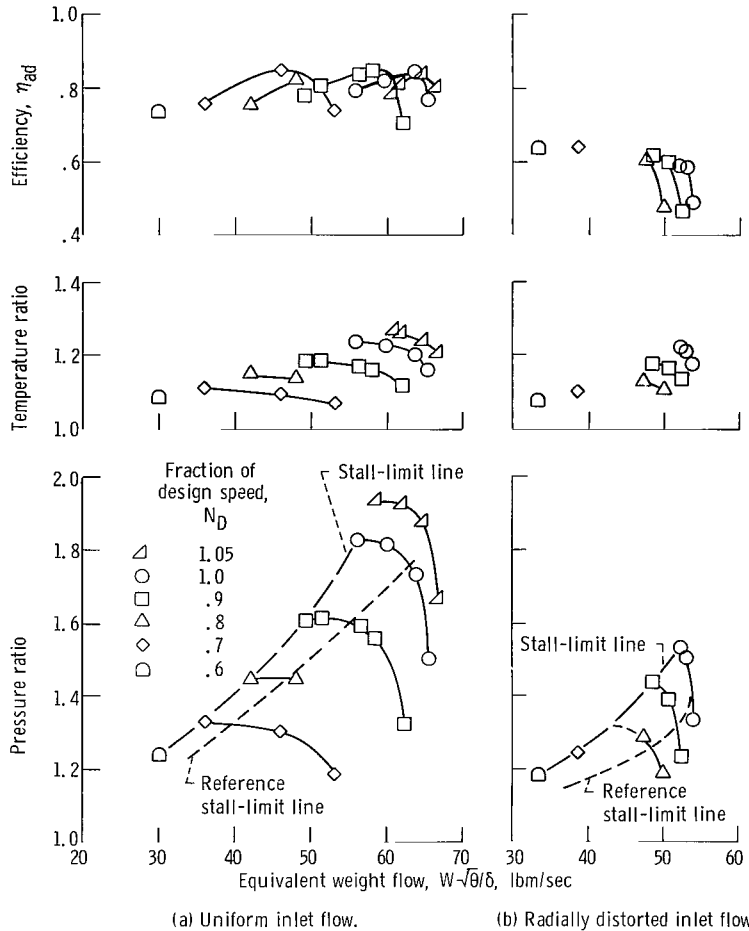
Figure 27. - Overall rotor performance for blade angle slotted casing with closed, shallow, and short slots.

    This casing treatment was the only one tested at a speed higher than design. At 1.05 N_D, a pressure ratio of 1.926 and an efficiency of 0.810 were obtained at the stall-limit point. Maximum efficiency was 0.834 at a weight flow of 64.81 pounds per second. The overall flow range was from 66.63 to 58.32 pounds per second.

    This configuration is the same as the previous configuration except for the shortening of the slot length, which was done by closing off a portion of a slot at the upstream and downstream edges. Thus, the casing treatment extended only over the center portion of the blade tip. The marked improvement in performance of the short slots over that of the long slots indicates that the blade angle casing benefits from minimizing axial recirculation of air upstream of the blade leading edge. It is possible that some of the other casing treatment configurations might also benefit by limiting the treatment to the casing over the center portion of the blade tip.

    <u>Radially distorted inlet flow</u>. - At design speed, the stall-limit point occurred at a

pressure ratio of 1.534 and a weight flow of 52.05 pounds per second. A maximum efficiency of 0.587 was also obtained at the stall point. The stall-margin increase over the reference casing was approximately 13.3 percent. There is a marked displacement of the stall-limit line from the reference line to lower flows and higher pressure ratios. This displacement is not as great at that obtained for the blade angle casings with long slots, but the pressure ratio and efficiency are higher.

COMPARISON OF ROTOR STALL-LIMIT LINES

In this section the stall-limit lines are compared for the following casings: reference solid, honeycomb, circumferentially grooved, skewed slotted (open and closed slots) and blade angle slotted (closed, shallow, and short slots). These casings were selected for comparisons because they gave the largest increases in stall margin at design speed with uniform inlet flow conditions. They also gave good increases in stall margin with radially distorted inlet flow. Table II summarizes the stall-margin in-

TABLE II. - SUMMARY OF SELECTED CASING-TREATMENT RESULTS

Configuration	Fraction of design speed	Uniform inlet flow		Radially distorted inlet flow	
		Percent stall margin over solid wall	Rotor maximum efficiency	Percent stall margin over solid wall	Rotor maximum efficiency
Reference solid casing	1.0	0	0.841	0	0.512
	.9	0	.829	0	.530
	.7	0	.823	0	.565
Skewed slotted casing with slots open to chamber	1.0	20.7	0.771	19.1	0.576
	.9	18.0	.807	27.5	.599
	.7	20.6	.806	22.5	.605
Skewed slotted casing with closed slots	1.0	15.3	0.793	15.0	0.571
	.9	13.1	.787	(a)	(a)
	.7	15.9	.787	(a)	(a)
Blade angle slotted casing with closed, shallow, and short slots	1.0	17.5	0.847	13.3	0.587
	.9	13.4	.849	16.2	.611
	.7	10.6	.848	15.4	(a)
Circumferentially grooved casing	1.0	13.5	0.849	5.9	0.583
	.9	9.3	.869	8.8	.622
	.7	1.1	.849	2.9	.626
Honeycomb casing with deep, small cells	1.0	12.1	0.817	3.9	0.528
	.9	11.9	.835	8.0	.550
	.7	4.9	.824	12.9	.589

[a]Not available.

creases and maximum efficiencies obtained with these casings for both uniform and radially distorted inlet flow. Also presented in this section is the rotor performance at design speed with circumferentially distorted inlet flow for the reference solid casing, the skewed slotted casing (closed), and the circumferentially grooved casing. An estimate of the stall-limit line displacement at design speed may be made by comparing the stall-limit points for the three casings.

Uniform Inlet Flow

The rotor stall-limit lines obtained with uniform inlet flow are shown in figure 28(a) for the selected casing treatments. For all of the selected casing treatments, the weight flow was lower and the pressure ratio was higher at the design speed stall-limit point than they were for the reference casing. The following casing treatments are listed in order of their ability to increase the stall margin over the reference casing at design speed: skewed slotted with open slots (20.7 percent), blade angle slotted with closed, shallow, and short slots (17.5 percent), skewed slotted with closed slots (15.3 percent) circumferentially grooved (13.5 percent), and honeycomb (12.1 percent). At 0.7 N_D, there is a rearrangement to the following order: skewed slotted with open slots (20.6 percent), skewed slotted with closed slots (15.9 percent), blade angle slotted (10.6 per-
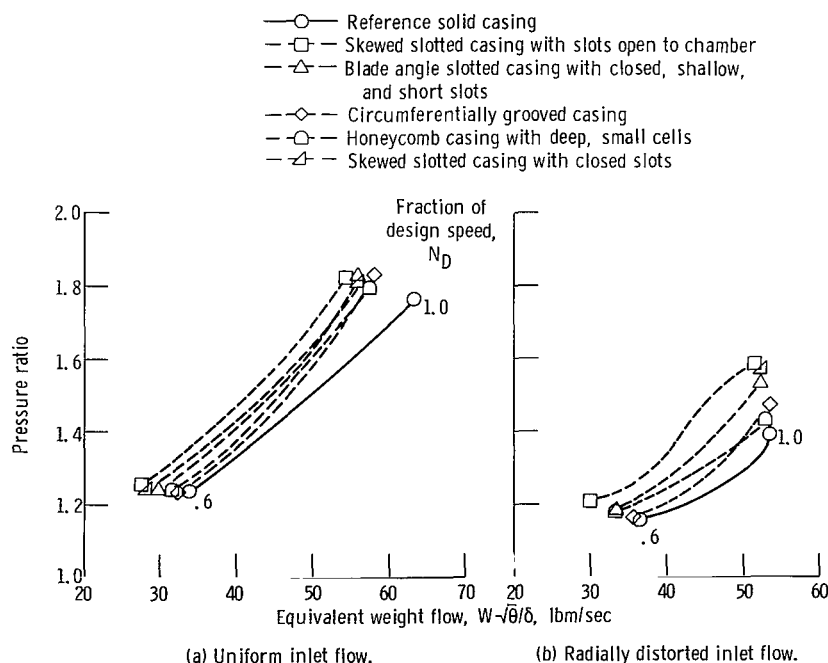

Figure 28. - Comparison of rotor stall-limit lines for selected casing treatments and reference casing.

cent), honeycomb (4.9 percent), and circumferentially grooved (1.1 percent).

The skewed slotted casing with open slots gave the largest displacement of the stall-limit line from the reference line at all speeds. However, its efficiency was lower than for the reference casing, particularly at design speed. The skewed slotted casing with closed slots also gave a good displacement of the stall-limit line at all speeds. It too was low in efficiency. The blade angle slotted configuration with closed, shallow, and short slots gave a good displacement of the stall-limit line at all speeds along with efficiency as high as that obtained with the reference casing. As pointed out in a previous section, its good performance extends to higher than design speed. The circumferentially grooved casing gave a good displacement of the stall-limit line at high speeds along with efficiencies that were slightly higher than those obtained with the reference casing. At low speeds, it displaced the stall-limit line very little. However, its simplicity and high efficiency makes it a desirable casing treatment for use at high speeds. The honeycomb casing treatment gave a good displacement of the stall-limit line at high speeds but gave only a fair displacement at low speeds. Its efficiency was slightly lower than that obtained with the reference casing.

Radially Distorted Inlet Flow

The rotor stall-limit lines obtained with the selected casing treatments and radially distorted inlet flow are shown in figure 28(b). At design speed, the weight flow at the stall-limit point for all the selected casing treatments are slightly less than that obtained for the reference casing. The stall-margin increases over the reference casing, however, result primarily from the higher pressure ratio obtained with the casing treatments. The following casing treatments are listed in order of their ability to increase the stall margin over the reference casing at design speed: skewed slotted with open slots (19.1 percent), skewed slotted with closed slots (15.0 percent), blade angle slotted with closed, shallow, and short slots (13.3 percent), circumferentially grooved (5.9 percent), and honeycomb (3.9 percent). For displacing the stall-limit line at $0.6 \, N_D$, the order would be the same except that the honeycomb would come before the circumferentially grooved. The maximum efficiencies obtained for all the casing treatments were higher than that obtained for the reference casing.

Circumferentially Distorted Inlet Flow

Only the circumferentially grooved casing, the skewed slotted casing with closed slots, and the reference casing were tested with circumferentially distorted inlet flow.
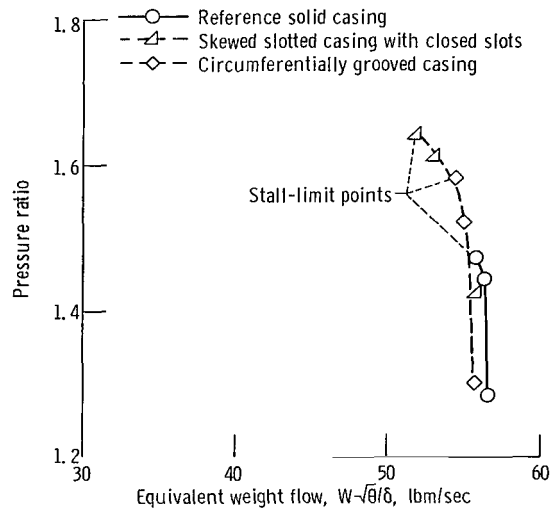
Figure 29. - Comparison of stall-limit points for selected casing treatments and reference casing with circumferentially distorted inlet flow.

Data were taken only at design speed. The performance curves for the reference casing and the two casing treatments are presented in figure 29. An estimate of the stall-limit line displacement from the reference lines may be made by comparing the stall-limit points for the three casings. The skewed slotted casing gave a stall-margin increase over the reference casing of 19.7 percent. The maximum efficiency was 0.622 as compared with 0.595 for the reference casing. The circumferentially grooved casing gave a stall-margin increase over the reference casing of 10.7 percent. The maximum efficiency was 0.671 as compared with 0.595 for the reference casing. For both casing treatments, the performance improvement at design speed was greater than that obtained for the same casing treatments with radially distorted inlet flow.

CONCLUDING REMARKS

Although the casing treatment evaluation tests presented herein were limited to one test rotor, a number of general observations may be made.

The test rotor selected for this investigation was more highly loaded in the tip region than at other portions of the blade span (ref. 3). Thus for this rotor rotating stall probably initiates in the blade tip region. Tip casing treatment might be expected to work best with this type of rotor by delaying the onset of rotating stall in the blade-tip regions.

For some of the casing treatments, stall-margin increases were obtained with efficiencies as high or slightly higher than those obtained with the solid reference casing. Thus, it may be desirable to consider casing treatment in the original rotor design con-

cept. A combination of a rotor designed to be tip critical (highly loaded in tip regions) and casing treatment over the rotor might give better overall performance than a conventionally designed rotor without casing treatment.

The casing treatment evaluation tests showed that several geometrically different casing treatments gave stall-margin increases over a reference solid casing. However, the characteristics of each treatment were different. The skewed slotted casing gave excellent increases in stall margin at all speeds, but was low in maximum efficiency, particularly at design speed. The blade angle slotted casing with closed, shallow, and short slots gave good increases in stall margin at all speeds with maximum efficiencies as high as those obtained with the reference solid casing. The circumferentially grooved casing gave a good increase in stall margin at design speed but very little increase at low speeds. However, its simplicity along with its maximum efficiencies, as high as or slightly higher than those obtained with the reference solid casing, make it a good casing treatment at high speeds. Thus, it may be desirable to choose a casing treatment to best fit the requirements of a given compressor application.

The modifications made to shorten the slots in the blade angle slotted configuration indicate that the casing treatment need extend only over a portion of the blade tip section. Thus, it would be of interest to evaluate the performance of the test rotor with shortened skewed slots as the casing treatment. Also, removing some of the grooves near the leading and/or trailing edges in the circumferentially grooved casing might improve still further the performance of the rotor with this casing treatment.

The slotted casings and the circumferentially grooved casing were fabricated with approximately two-thirds of the treated area as open area. Good increases in stall margin were obtained with these casing treatments. The two perforated casings with 30 and 40 percent open area gave little or no increase in stall margin. There may be an optimum value of open area to obtain the best performance, but a more detailed investigation would be required to establish such a value.

Good stall-margin improvement was obtained with both the skewed and blade angle slotted configurations in which the slot was closed. The honeycomb casings were also closed and gave a good stall-margin increase. Thus, it appears that a plenum chamber behind the slots is not necessary.

The tests were inconclusive as to the effect of tuning the casing treatment. Tuning seemed to have had no effect on the honeycomb casings. However, the tuned configuration of the skewed slotted casing (open slots) was slightly better than the untuned configuration (closed slots). The blade angle slotted casing with shallow and long slots performed very poorly (with uniform inlet flow); with shallow and short slots it performs very well. Both configurations were tuned to blade passing frequency at $0.9 \, N_D$. At least it appears that tuning has no detrimental effects; for the present it seems to be a reasonable method for selecting the passage depth.

SUMMARY OF RESULTS

A series of evaluation tests were made to determine the effects of a number of porous casing on the performance of an axial flow compressor rotor. The effectiveness of the casing treatments was judged primarily by their ability to increase the rotor stall margin by displacing the rotor stall-limit point to lower flow rates while maintaining or increasing the pressure ratio at any particular speed. The tests were conducted with uniform, radially distorted, and circumferentially distorted inlet flow. The following results were obtained from the tests.

1. The skewed slotted casing with open slots gave the greatest displacement of the stall-limit line of any of the casing treatments tested. With uniform inlet flow, stall margin increases of 20.7, 18.0, and 20.6 percent were realized at 1.0, 0.9, and 0.7 of design speed, respectively. Corresponding maximum efficiencies were 7.0, 2.2, and 1.7 percentage points lower than those obtained with the reference solid casing. With radially distorted inlet flow stall-margin increases of 19.1, 27.5, and 22.5 percent were obtained for these speeds.

2. The skewed slotted casing with closed slots also gave a good displacement of the stall-limit line. With uniform inlet flow, stall-margin increases of 15.3, 13.1, and 15.9 percent were obtained at 1.0, 0.9, and 0.7 of design speed, respectively. Maximum efficiencies were 4.8, 4.2, and 3.6 percentage points lower than those obtained with a solid casing. With radially distorted inlet flow, a stall-margin increases of 15.0 percent was obtained at design speed.

3. The blade angle slotted casing with closed, shallow, and short slots gave a good displacement of the stall-limit line, whereas this casing with deeper and longer slots gave no improvement. Stall-margin increases of 17.5, 13.4, and 10.6 percent were obtained with uniform inlet flow at 1.0, 0.9, and 0.7 of design speed, respectively. Maximum efficiencies were as high as or slightly higher than those obtained with a solid casing. With radially distorted inlet flow, stall-margin increases of 13.3, 16.2, and 15.4 percent were obtained.

4. The circumferentially grooved casing treatment with uniform inlet flow gave a good displacement of the stall-limit line to lower flow rates at high speeds but very little displacement at low speeds. Maximum efficiencies were slightly higher than those obtained with a solid casing. Stall-margin increases of 13.5, 9.3, and 1.1 percent were obtained at 1.0, 0.9, and 0.7 of design speed, respectively. Corresponding stall-margin increases of 5.9, 8.8, and 2.9 percent were obtained for radially distorted inlet flow.

5. The honeycomb configurations (deep, shallow, and large or small cell) all gave approximately the same rotor performance with uniform inlet flow. There was a good displacement of the stall-limit line to lower flow rates and stall-margin increases of 12.1, 11.9, and 4.5 percent were obtained at 1.0, 0.9, and 0.7 of design speed, respec-

tively. Maximum efficiencies were slightly lower than for the solid casing. Corresponding stall margin increases with radially distorted inlet flow were 3.9, 8.0, and 12.9 percent.

6. The axially slotted casing treatment gave a good displacement of the stall-limit line at speeds as high as 0.9 of design speed but no displacement at design speed. The results of the tests are inconclusive as the slots were damaged during the tests; it is possible that the damaged slots may have had decreased effectiveness when the design-speed test was run.

7. The perforated casings with either 0.0625- or 0.125-inch-diameter holes gave essentially the same performance as the reference solid casing with little or no displacement of the stall-limit line.

8. For circumferentially distorted inlet flow, the limited data obtained indicate that substantial increases in stall margin may be obtained by the use of casing treatment.

Lewis Research Center,
　　National Aeronautics and Space Administration,
　　　　Cleveland, Ohio, July 15, 1971,
　　　　　　720-03.

REFERENCES

1. Koch, C. C.: Experimental Evaluation of Outer Case Blowing or Bleeding of Single Stage Axial Flow Compressor. Part VI. Rep. R69AEG256, General Electric Co. (NASA CR-54592), Jan. 30, 1970.

2. Bailey, Everett E.; and Voit, Charles H.: Some Observations of Effects of Porous Casings on Operating Range of a Single Axial-Flow Compressor Rotor. NASA TM X-2120, 1970.

3. Ball, Calvin L.; Janetzke, David C.; and Reid, Lonnie: Performance of 1380-Foot-Per-Second-Tip-Speed Axial-Flow Compressor Rotor With Blade Tip Solidity of 1.5. NASA TM X-2379, 1971.

"The aeronautical and space activities of the United States shall be conducted so as to contribute . . . to the expansion of human knowledge of phenomena in the atmosphere and space. The Administration shall provide for the widest practicable and appropriate dissemination of information concerning its activities and the results thereof."

— NATIONAL AERONAUTICS AND SPACE ACT OF 1958

NASA SCIENTIFIC AND TECHNICAL PUBLICATIONS

TECHNICAL REPORTS: Scientific and technical information considered important, complete, and a lasting contribution to existing knowledge.

TECHNICAL NOTES: Information less broad in scope but nevertheless of importance as a contribution to existing knowledge.

TECHNICAL MEMORANDUMS: Information receiving limited distribution because of preliminary data, security classification, or other reasons.

CONTRACTOR REPORTS: Scientific and technical information generated under a NASA contract or grant and considered an important contribution to existing knowledge.

TECHNICAL TRANSLATIONS: Information published in a foreign language considered to merit NASA distribution in English.

SPECIAL PUBLICATIONS: Information derived from or of value to NASA activities. Publications include conference proceedings, monographs, data compilations, handbooks, sourcebooks, and special bibliographies.

TECHNOLOGY UTILIZATION PUBLICATIONS: Information on technology used by NASA that may be of particular interest in commercial and other non-aerospace applications. Publications include Tech Briefs, Technology Utilization Reports and Technology Surveys.

Details on the availability of these publications may be obtained from:

SCIENTIFIC AND TECHNICAL INFORMATION OFFICE

NATIONAL AERONAUTICS AND SPACE ADMINISTRATION
Washington, D.C. 20546